Article

Transformed Corrugated Shell Units Used as a Material Determining Unconventional Forms of Complex Building Structures

Jacek Abramczyk

Department of Architectural Design and Engineering Graphics, Rzeszow University of Technology, Al. Powstańców Warszawy 12, 35-959 Rzeszów, Poland; jacabram@prz.edu.pl

Abstract: This article is an insight into interdisciplinary topics in the field of civil engineering, morphology, architecture, mechanics, and computer programming. A novel method for shaping unconventional complex roofs in which regular folded units transformed into various shells are used as a complex substitute material is proposed. The original method's algorithm for building systems of planes defining diversified polyhedral networks in the three-dimensional space by means of division coefficients of the subsequently determined vertices is presented. The algorithm is based on the proportions between the lengths of the edges of the reference network, the location and shape of the ruled shell units included in the designed complex roof structure, so it is intuitive. The shell units are made up of nominally flat folded sheets transformed effectively into shell forms whose static-strength properties are controlled by geometric quantities characteristic of ruled surfaces. The presented original approach to the shaping of the shell roof structures determining specific complex building forms allows us to go beyond the limitations related to the orthotropic structure of the folded roof sheeting and the shape transformations.

1. Introduction

Since the transverse flexural stiffness and torsional stiffness of a nominally flat thin-walled steel sheet of open profile and folded in one direction are small, then a small load applied perpendicularly to the neutral surface of the sheet causes a significant initial shape change. The loaded sheets connected by their longitudinal edges into a nominally flat single strip are spread on at least two mutually skew directrices to change their forms from flat into ruled shells, depending on the shape and the mutual position of the directrices [1] (Figure 1).

Figure 1. Experimental folded shell sheeting supported by two curvilinear skew directrices.

In order to reduce the initial stresses resulting from the aforementioned shape transformations, each fold tends to balance the tensile stresses appearing at both fold's transverse ends, with the compressive stresses appearing at a half along the fold's length. If a freedom of the fold's changes manifesting especially in the fold's width increments is ensured during spreading and fixing all folds to the roof directrices, then the folds tend to obtain such shell forms that their longitudinal axes remain straight lines and their contraction appears at a half-way along the length of each shell fold. The geometry of all subsequent cross-sections of each transformed fold variously changes along the fold's length, so that each fold reaches the maximum contraction and the maximum height at a half along its length.

Since the length of the thin-walled steel sheets is relatively small and the aforementioned geometric and structural limitations of the effectively transformed sheets are very important boundary conditions, it is impossible to obtain a single smooth shell roof of a medium span [1,2] (Figure 2). Therefore, the complete transformed shell sectors are joined by means of their transverse edges into ribbed structures, so that the shape of each shell sector is characterized by a contraction passing through the halves of all folds at their length to optimize the initial stresses [3].

(a) **(b)**

Figure 2. Complex shell structure roofing an experimental hall: (**a**) an outside view; (**b**) an inside view.

For scientific research, experimental tests and computer simulations are carried out by Abramczyk [1,4] (Figure 3), where the transformed experimental folded sheeting is accurately modeled with computational thin-walled folded sheeting. The geometry, strength and stability of these models are analyzed by Abramczyk [5], using advanced dynamic incremental non-linear methods described by Bathe [6].
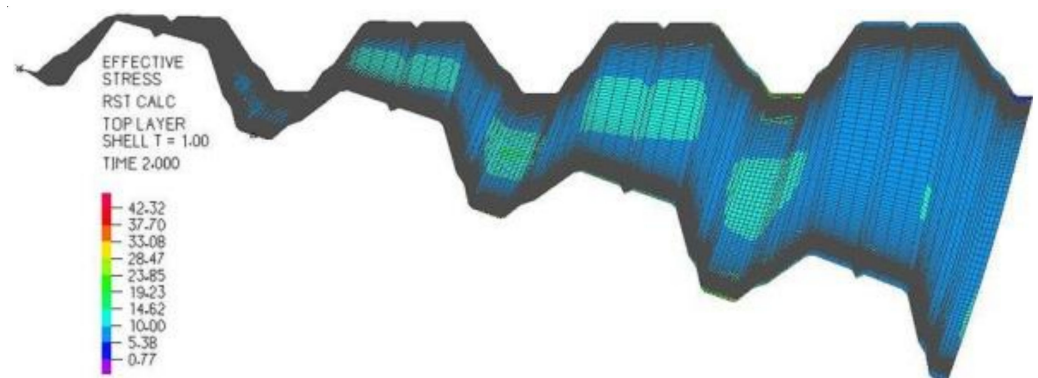
Figure 3. The accurate computational mechanical model of an elastically transformed sheet and the graphical expression of the "effective" stresses in MPa on its top surface.

2. Critical Analysis of the Present Knowledge

The complete thin-walled folded shells transformed into central sectors of hyperbolic paraboloids were investigated by many researchers. The main geometric and mechanical properties of folded sheeting deformed into corrugated hyperbolic paraboloid shells were presented by Nilson [7]. The Winter's team [8] confirmed Nilson's results and expanded on the scope of the performed tests and analysis. Parker analyzed structures composed of a few quarters of right hyperbolic paraboloids made of two layers of sheets located orthogonally in the same shell.

McDermott [9] described the behaviour of a central sector of a folded steel hyperbolic paraboloid stiffened with a circumferential frame. Parallel studies related to the static-strength work single and complex hyperbolic paraboloid shells were conducted by Egger et al. [10] based on the conventional analysis and analytical calculations of strength and critical loads. Gergely et al. [11] carried out a detailed analysis of the static-strength work of the single and complex profiled hyperbolic paraboloid shells composed of two orthogonal layers, which enables these research studies to analyze the shells as isotropic.

Gioncu and Petcu [12] developed the novel HYPBUCK computer program for calculating the critical loads. Davis and Bryan [13] pointed out the most important geometric and mechanical characteristics of the transformed shell folds, to make it easier for the designer to shape the transformed shells. Finally, they stated that theoretically it is possible to shape many different types of the transformed folded shell sheeting. Practically, it is possible to build only cylindrical and shallow corrugated hyperbolic paraboloid roofs due to the available engineering technology. In summary, all the investigated shells underwent forced shape transformations, causing relatively big initial stresses, because the fold's longitudinal axes were adapted to the selected rulings of the adopted hyperbolic paraboloids. Therefore, the initial stresses had to be restricted, for example, by limiting the transformation degree. As a result, only shallow hyperbolic-paraboloid shells called hypars can be created (Figure 4).

(**a**)　　　　　　　　　　　　　　　　　　　　　　　(**b**)
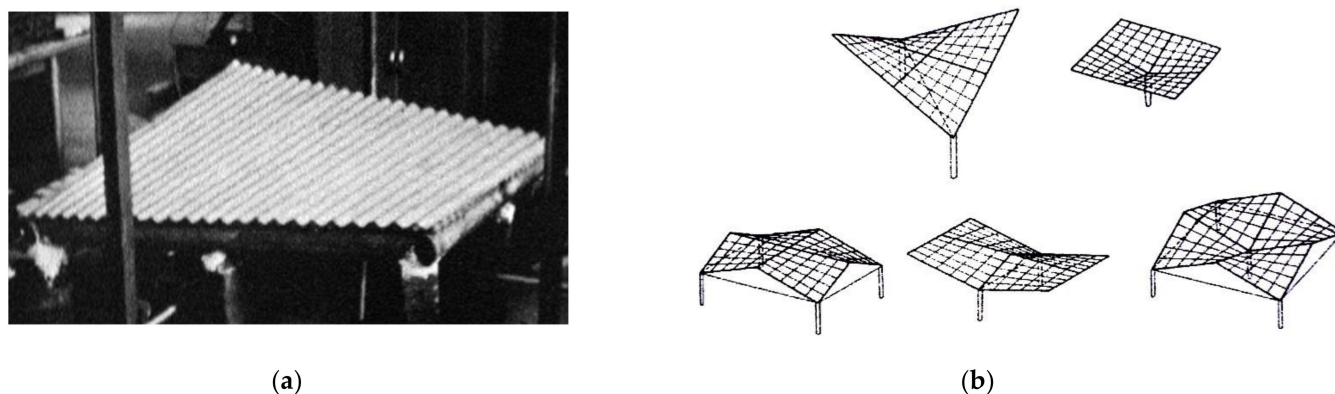
Figure 4. Two symmetric experimental hyperbolic paraboloid shells: (**a**) a complete shell; (**b**) umbrella structures of four quarters.

Biswas and Iffland [14] presented a few concepts of shaping continuous regular roof structures composed of many identical hyperbolic paraboloid segments made up of transformed folded steel sheets. They arranged many complete shell sectors on a sphere to increase the span of the designed free form building.

The thin-walled corrugated shell steel roofs transformed freely are shaped by Reichhart [15] and simply modeled with various right hyperbolic paraboloids (Figure 5) and other deeply ruled surfaces [16]. For geometric engineering developments, each shell sheeting can be modeled with a smooth sector of a ruled undevelopable surface called a warped surface [1] (Figure 1) including hyperbolic paraboloid [17] (Figure 2).

Figure 5. The external views of two opposite elevations of the experimental hall at a university roofed with the shell structure: (**a**) the roof structure; (**b**) the south side of the entire building.

In order to create a method for shaping corrugated shells transformed rationally, Abramczyk has proposed a condition requiring the contraction of a single shell to pass halfway along the length of each shell fold [1] (Figure 3). Abramczyk's method employs some specific geometric properties of regular warped surfaces, primarily their lines of striction. The second condition utilized by Abramczyk relates to determining certain surface areas of the created smooth shell models corresponding to the compressing and stretching zones of each transformed fold [3]. These two conditions are based on the results of his experimental tests and computer simulations (Figures 1 and 3).

The quarters of the hyperbolic paraboloid shells are often arranged symmetrically in different configurations to increase the expected roof spans. In order to create diversified free form building structures roofed with complex corrugated shells characterized by medium spans, Prokopska and Abramczyk [18,19] analyzed the so-called reference tetrahedrons to model a complete free form covered with oblique plane elevations and roofed with many transformed complete corrugated shell sectors arranged regularly in the three dimensional space [20].

Each single shell segment is modeled by Abramczyk for the engineering developments [1] with a sector of a warped surface [21] (Figure 6a), limited by a closed spatial line composed of four segments contained in the planes of a so-called reference network [22]. The planes of the reference network divide the complete shell segments of the designed shell roof structure. They are helpful in defining roof directrices (Figure 6b). In the present article, all directrices e and f are straight sections.
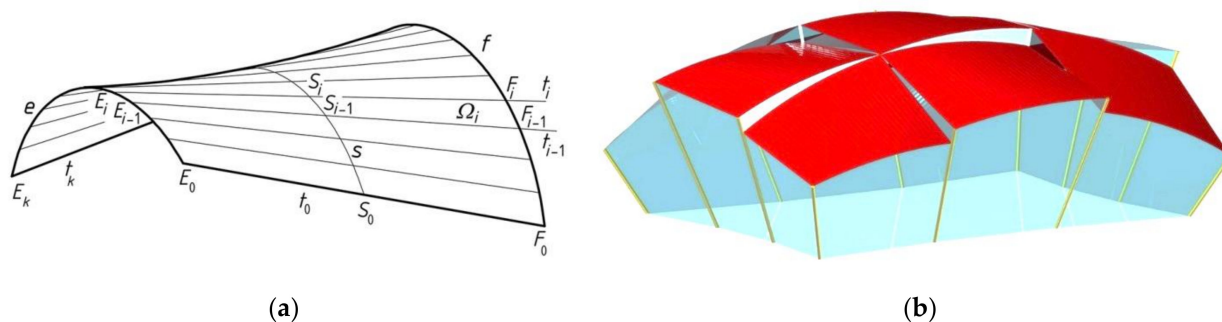
Figure 6. (**a**) A simplified geometric smooth model of a complete corrugated shell sheeting; (**b**) A simplified geometric model of a building free form roofed with complex corrugated shell sheeting structure.

Abramczyk [23] developed a method for shaping axis symmetric polyhedral networks based on rigid motions of all vertices of these networks (Figure 7). Four adjacent planes of each reference network limit one tetrahedral mesh. A parameterization of the reference networks enables one to shape various configurations of attractive complex building free forms and innovative structural systems intended for these free forms by means of computer technique.
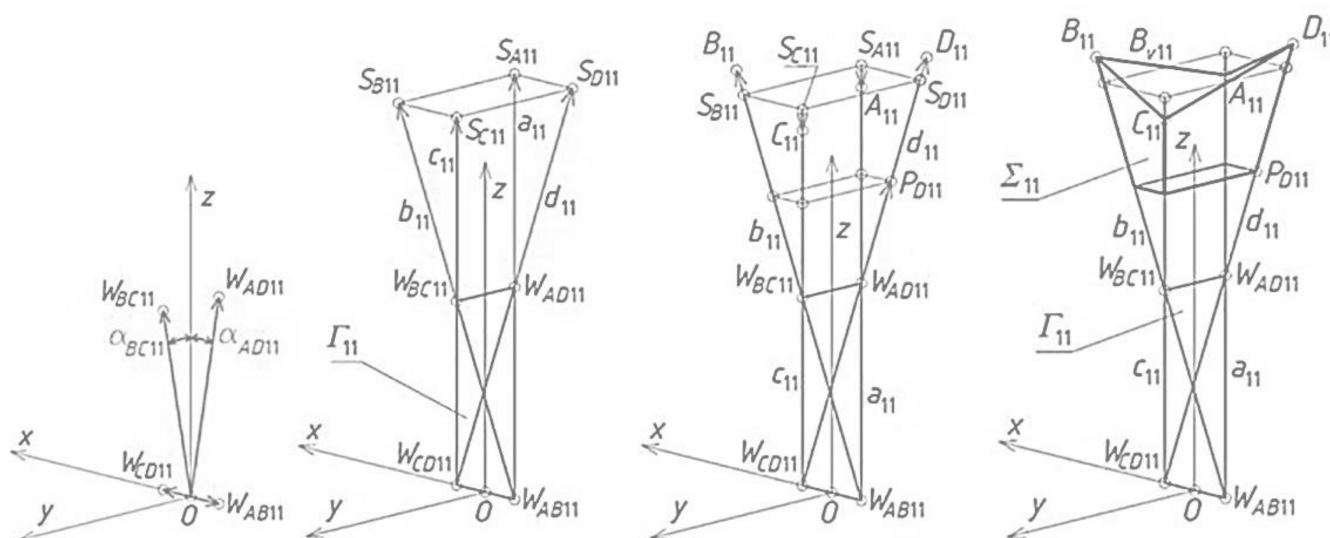

Figure 7. Stiff motions: translations and rotations for creating meshes Γ_{11}, B_{v11} and $\sum_{11}$.

The above-mentioned method allows one to transform the shapes of various types of building structures proposed by Abdel and Mungan [24] and Saitoh [25]. Free-form shell bar structures are presented by Obrębski [26]. Structural bar systems for several types of the corrugated roofs were developed by Rębielak [27]. Free-form buildings and their constructions were analyzed by Reichhart [28] and Wei-Wen [29]. Samyn suggests interesting aluminium hypar forms [30].

The most general method of architectural shaping of polyhedral shell structures was developed by Pottmann et al. [31,32]. The designed geometry of these structures does not result from the orthotropic properties, rectangular shapes of the folded sheets and the shape transformations of the designed roof shells.

The folded steel sheeting transformed elastically or plastically can be used as a structural shell unit supporting appropriate roof covers [33]. The classical theory of elasticity proposed by Green and Lindsay has been extended by Marin et al. [34] to cover the theory of thermoelasticity for dipolar bodies. A specific method of unique solution of a mixed problem in the dynamical case is proposed using a reciprocal theorem [35]. These fundamental results were obtained under not very restrictive conditions.

3. The Aim and the Scope of the Research

The aim of this article is to present a novel method for shaping unconventional complex shell roof structures whose various complete folded shell segments are used as a complex substitute material. The unit segments of a similar ruled form are located in the three-dimensional space in an orderly and effective manner using a reference regular surface and an innovative regular polyhedral network whose straight edges are normal to this reference surface.

The presented parametric development of the specific polyhedral reference networks enables one to computationally shape diversified unconventional complex building free forms roofed with regular structures composed of many different shell segments made up of nominally flat thin-walled steel folded sheets transformed into various corrugated

shell shapes. Simplified geometric models of the complete roof shells created by means of the method as smooth sectors of warped surfaces are sufficient for most engineering developments. These models can be determined by means of the reference and eaves networks investigated in the present article.

The method's algorithm must be supported by computer technology due to the accessibility of the method for designers. This is why a few novel computer applications were written in one of the CAD programming languages. The important feature of the algorithm is that the proposed reference networks enable an intuitive and automatic modification of the obtained results to adapt these networks to the geometric and static-strength characteristics of the transformed folded sheets and the required geometric boundary conditions. These conditions are related to some initially adopted proportions between the dimensions of all main elements of the designed building and the shape and mutual position of all pairs of the designed roof directrices.

The description and the computer implementation of the presented algorithm, helpful in searching for possible and acceptable parametric configurations and modifications of the reference networks, have led to rational solutions related to: (1) attractive forms of the designed complex building forms, in particular multi-plane folded facades and multi-segment shell roof sheeting, (2) satisfactory stability and the smallest possible effort causing by the investigated shape transformations, and (3) rationality of shaping of bar structural systems intended for the complex building forms.

4. The Method's Concept

The process of shaping the built environment by means of diverse unconventional building forms requires one to solve many interdisciplinary issues in the field of town planning, architecture, morphology, civil engineering, constructions and computer support. Each issue is considered at different levels of accuracy, which further complicates the process of conducting the relevant analysis. The complex design process must therefore be divided into many steps related to the function, arrangement and type of the components of the building shaped, as well as the level of the modeling accuracy and execution of these elements.

The relation between the formation of the urban space and the social experience of the human self must be taken into account [36]. The formation of the space investigating its physical form and cultural patterns into a whole spatial system is very important.

The design syntax of urban greenways should also be explicitly discussed. In this way, mathematics-based graph studies to analyze patterns and shapes, photography based thermal, material and morphology studies, and section analyses to make imagery-derived deductions on the design syntax are carried out [37].

The morphological shaping of buildings plays a significant role in the design process, by using features specific for architectural, industrial and structural design [38]. Morphology is a study of the forms taking account of the adopted interrelationships between the function, structure, internal and external texture, static-strength work and comfort conditions ascribed to the designed building object.

In each of the above mentioned aspects of the design process, a strict ordering of the objects characteristic for the considered step must be carried out. Therefore, according to the deliberated step, the general model is divided into many consistent individual elements and then into sub-elements arranged in a strictly defined order. These elements are adapted to the utilized concept, in accordance with the production technology and the assembly technique.

Thorough research and tests allow one to create appropriate geometric and static-strength models used in the search and development of the new concepts and techniques. The created unconventional new forms result from various innovative approaches to the shaping and ordering of their individual elements, for example in the three-dimensional Euclidean space.

Systematic morphology is defined by Eekhout as "the study of the system, rules and principles of form has led to the interpretation of the study of the geometry of regular three-dimensional bodies or forms, usually known as polyhedra." [38]. Analogous systems of planes called polyhedral reference networks are used in the present article. These are sums of many regular tetrahedrons arranged regularly in the three-dimensional space.

Wester defined structural morphology as "the Study of Form" [39]. A detailed description of the issues related to the morphology of the structure is presented by Qingpeng [40]. In this article, the study is limited to the geometric shaping of complex building structures roofed with free-form transformed corrugated shell structures arranged regularly in the three-dimensional space. The arrangement of the complete roof shell sectors is carried out by means of plane systems called polyhedral reference networks. The individual planes of each system separate single roof shells and contain the directrices of these shells. The diversification of the shape and mutual position of each pair of the adjacent directrices enables one to shape various innovative transformed forms of the complete corrugated shells.

The following factors have a decisive impact on the geometric properties of the investigated reference networks: (1) the regularity of the shapes and arrangement of the designed roof structures, (2) the rectangular shapes of the utilized folded sheets connected by their longitudinal edges into a single transformed strip, respectively, (3) the shape and mutual position of the roof directrices supporting each individual transformed shell segment, and (4) multi-wall character of the shaped complex facades. The assumed multi-segment nature of each roof structure Ω divided by the specific sets of planes allows all individual shells Ω_{ij} to be arranged by joining together along their transverse edges in relation to the fold directions. This way of connection results in specific ribbed roof structures.

Two adjacent shells of a roof structure can be connected along common eaves lines, including directrices (Figures 2 and 5), or separated by flat window areas, allowing the sun rays to illuminate the building interior. This method allows the designer to shape freely attractive free forms of the roof structures (Figure 6b). In the last case, the roof directrices of two adjacent shells are contained in the same plane, which forced development of a specific method for creating the special systems of these planes called polyhedral reference networks.

The quadrilateral nature of each closed edge line B_{vij} limiting each complete transformed roof shell Ω_{ij} results in that each reference network Γ is composed of meshes Γ_{ij} restricted by tetrads of planes. Due to the rectangular characteristics of the individual sheets and their strips, the meshes are built as specific reference tetrahedrons whose four walls contain four single segments of the edge line B_{vij} of each single shell Ω_{ij}. Thus, all B_{vij} are closed spatial quadrangles whose all four apex angles are close to right angles.

As a rule, the complete shell segments are variously transformed, because they take relatively different forms depending on the shape and mutual position of their roof directrices adapted to the diversified curvature of the whole roof shell structure. Many special regular single shell sectors Ω_{ij} and complete free forms $\sum_{ij}$ should be located in one polyhedral network mesh Γ_{ij} (Figure 8a). Thus, the respective façade walls, side edges, roof directrices and eaves segments are included in the tetrad of planes of each Γ_{ij}. The most general type of the tetrahedral meshes Γ_{ij} was adopted in the further analysis (Figure 8b). Every two adjacent planes of the same mesh Γ_{ij} intersect in a side edge a_{ij}, b_{ij}, c_{ij} or d_{ij}, however, two of its opposite planes intersect in one axis u_{ij} or v_{ij}. The side edges and axes are defined by means of four vertices W_{ABij}, W_{CDij}, W_{ADij} and W_{BCij}, adopted initially or created previously for Γ_{ij} (Figure 8b).

Subsequently, tetrads of points S_{Aij}, S_{Bij}, S_{Cij} and S_{Dij} are determined on four side edges a_{ij}, b_{ij}, c_{ij}, d_{ij} in relation to four adopted vertices W_{ABij}, W_{CDij}, W_{ADij} and W_{BCij} of Γ_{ij}, ($i = 2$, $j = 1$) (Figure 8a). The constructed points are the vertices of a quadrangle $S_{Aij}S_{Bij}S_{Cij}S_{Dij}$ constituting a plane mesh of an auxiliary multi-plane edge net determining a reference surface ω_r. In relation to the reference surface ω_r, four vertices A_{ij}, B_{ij}, C_{ij}, D_{ij} of the quadrilateral eaves net B_{vij} are determined. Other tetrads of points P_{Aij}, P_{Bij}, P_{Cij} and P_{Dij} defining a flat horizontal base of the sought-after free form $\sum$ are also constructed in

relation to four vertices W_{ABij}, W_{CDij}, W_{ADij} and W_{BCij}. The complex free form $\sum$ determined by the reference network Γ is a sum of all individual free forms $\sum_{ij}$ roofed with Ω_{ij}.
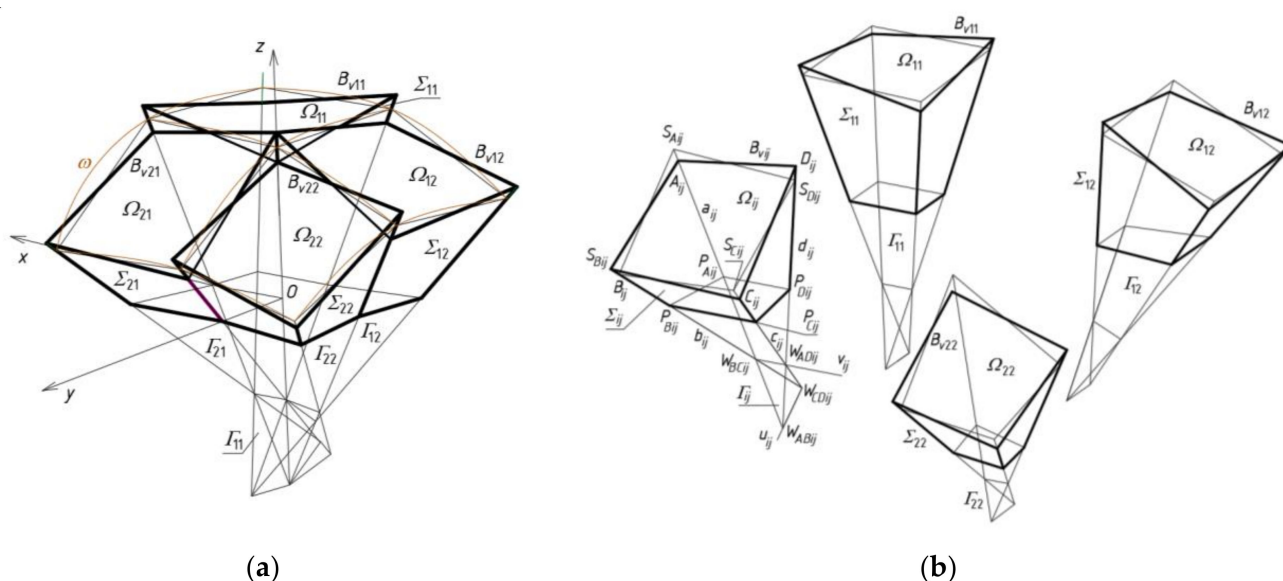
Figure 8. Creating complex building free form by means of a polyhedral reference network consisting of tetrahedral meshes divided by common sides: (**a**) the obtained Γ and $\sum$ after setting up Γ_{ij} and $\sum_{ij}$, with each other; (**b**) Γ_{ij} and $\sum_{ij}$ before setting.

To construct the subsequent shell sectors Ω_{ij} of different curvature in two orthogonal directions, the axes u_{ij} and v_{ij} must be mutual skew. The greater the curvature diversity of Ω_{ij} in two orthogonal directions, the greater the distance between the u_{ij} and v_{ij} axes must be adopted. To build the diversified shells Ω_{ij} as sectors of warped surfaces, many pairs of directrices must be modeled with the help of skew straight or curved lines contained in opposite walls of each tetrahedron Γ_{ij}.

The parameterization proposed in the present article regarding the geometric process of shaping such free forms $\sum$ is based on an adoption of a finite set of independent variables entering into the proposed novel computer application in the form of division coefficients of the respective pairs of the investigated Γ's vertices. The algorithm of the activities leading to the creation of Γ and $\sum$ is presented in Section 5.

5. Results—The Methods Algorithm

The first step of the method's algorithm relates to the determination of all vertices of the subsequent reference tetrahedrons Γ_{ij}, constituting the meshes of a reference network Γ. The first mesh Γ_{11} is created so that the positions of its four vertices W_{AB11}, W_{CD11}, W_{AD11} and W_{BC11} are defined. For that purpose, a global coordinate system $[x,y,z]$ with the origin O was taken (Figure 9a). A first set of the initial data concerning the creation of Γ_{11} is formed from the coordinates of these vertices. A few ways of determination of the vertices belonging to the investigated reference networks were developed by Abramczyk [1,17,21]. If we want a sought-after mesh to be symmetric, then its vertices must be arranged either symmetrically, in accordance with the principal planes (x,z) and (y,z), or in these planes. After defining the vertices W_{AB11}, W_{CD11}, W_{AD11} and W_{BC11}, we can determine four straight side edges a_{11}, b_{11}, c_{11} and d_{11} of Γ_{11}.

The second reference tetrahedron Γ_{12} is located along the (x,z)-plane in one of two principal orthogonal directions relative to Γ_{11} (Figure 9b). Its vertex W_{AB12} is identical to W_{CD11} introduced previously, so the second set of the initial data is composed of the coordinates of three other vertices W_{CD12}, W_{AD12} and W_{BC12} of Γ_{12}. These vertices can be determined as follows. The positions of the vertices W_{BC12}, W_{AD12} have to be defined on two side edges $b_{12} = c_{11}$, $a_{12} = d_{11}$, by means of two division coefficients of the pairs

(W_{CD11}, W_{BC11}) and (W_{CD11}, W_{AD11}) by these vertices. The division coefficients constitute the elements of the second set of the initial data instead of the coordinates of these points.
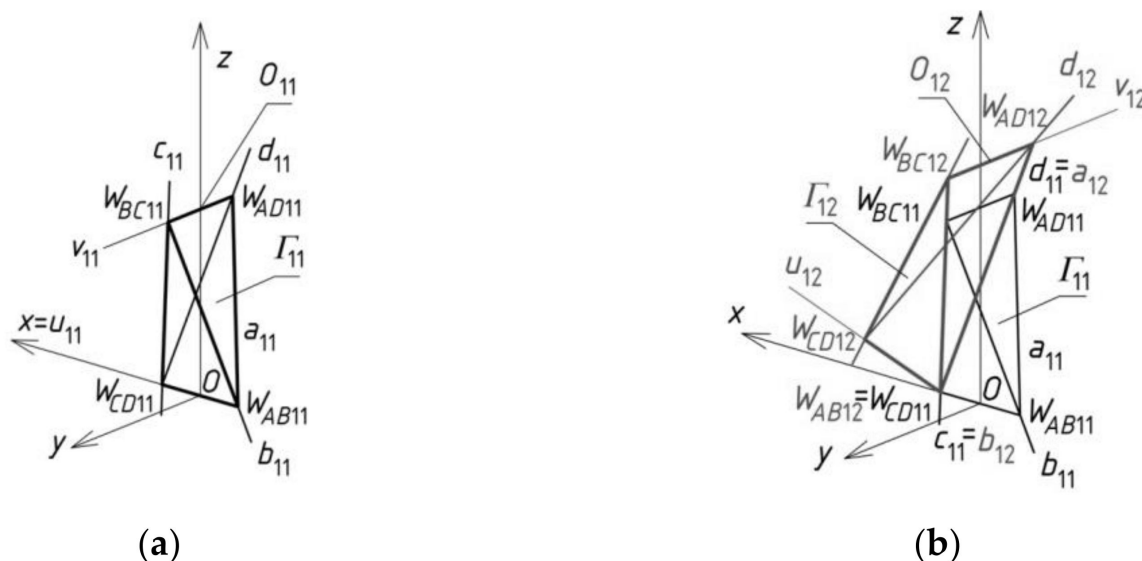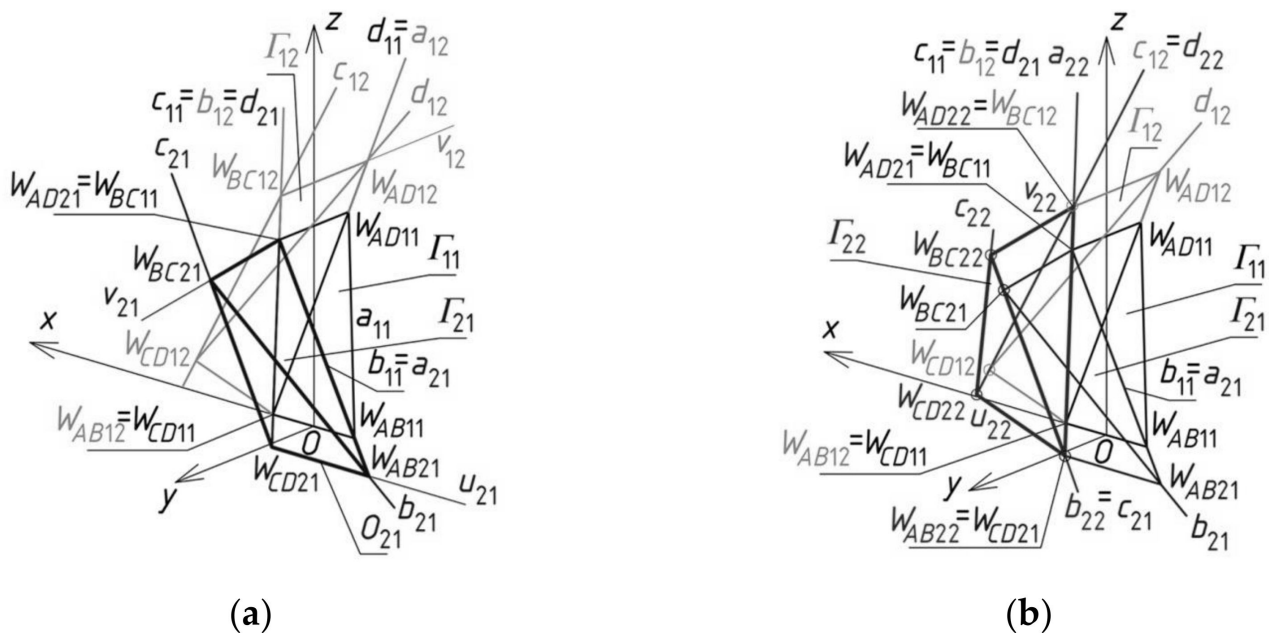

Figure 9. The results of two initial steps of the method's algorithm used for creating Γ: (**a**) Γ_{11}; (**b**) Γ_{12}.

The position of vertex W_{CD12} is obtained as a result of a rotation of the triangle $W_{AB12}W_{BC12}W_{AD12}$ about the axis $v_{12}(W_{AD12}, W_{BC12})$ into the position of the triangle $W_{CD12}W_{BC12}W_{AD12}$ (Figure 9b). If Γ_{12} is to be symmetrical towards the (x,z)-plane, W_{BC12} and W_{AD12} have to be identical to each other with respect to this plane. The point O_{12} helpful in programming, is the middle point of $W_{AD12}W_{BC12}$. Four vertices W_{AB12}, W_{CD12}, W_{AD12} and W_{BC12} determine four straight side edges: a_{12}, b_{12}, c_{12} and d_{12} of Γ_{12}. The remaining tetrahedrons Γ_{1j} (for $j > 2$) arranged symmetrically along the (x,z)-plane are determined in an analogous manner.

The third reference tetrahedron Γ_{21} is located in the second of two principal orthogonal directions of Γ_{11}, that is, along the (y,z)-plane (Figure 10a). The third set of the initial data is composed of the coordinates of only three vertices W_{AB21}, W_{CD21} and W_{BC21} of Γ_{21} because the other vertex $W_{AD21} = W_{BC11}$. The positions of the vertices W_{AB21} and W_{CD21} are defined on two side edges $a_{21} = b_{11}$, $d_{21} = c_{11}$ with the help of two division coefficients belonging to the third set of initial data instead of the coordinates of these points. The position of vertex W_{BC21} is obtained as a result of a rotation of the triangle $W_{AD21}W_{CD21}W_{AB21}$ about the axis $u_{21}(W_{CD21}, W_{AB21})$ into the position of the triangle $W_{BC21}W_{CD21}W_{AB21}$. If (y,z) is to be the plane of symmetry of Γ_{21}, then W_{CD21} and W_{AB21} have to be isentical to each other in relation to this plane. In addition, the point O_{21}, helpful in programming, has to be taken as the middle point of $W_{CD21}W_{AB21}$. Four vertices—W_{AB21}, W_{CD21}, W_{AD21} and W_{BC21}—determine four straight side edges—a_{21}, b_{21}, c_{21} and d_{21} of Γ_{21}. The remaining tetrahedrons Γ_{i1} (for $i > 2$) arranged along the (y,z)-plane are determined in an analogous manner.

The fourth reference tetrahedron Γ_{22} is located diagonally in relation to Γ_{11} (Figure 10b). The fourth set of the initial data should be composed of the coordinates of only two vertices W_{CD22} and W_{BC22} because $W_{AD22} = W_{BC12}$ and $W_{AB22} = W_{CD21}$. The positions of W_{CD22} and W_{BC22} are defined on two side edges $d_{22} = c_{12}$, $b_{22} = c_{21}$ with the help of two division coefficients belonging to the fourth set of the initial data, instead of the coordinates of these points. Four vertices—W_{AB22}, W_{CD22}, W_{AD22} and W_{BC22}—determine four straight side edges a_{22}, b_{22}, c_{22} and d_{22} and two axes u_{22} and v_{22} of Γ_{22}. The remaining tetrahedrons Γ_{ij} (for $i,j > 2$) arranged diagonally in relation to Γ_{11} are determined in an analogous manner.

Figure 10. The results of further initial steps of the method's algorithm used for creating Γ: (**a**) Γ_{21}; (**b**) Γ_{22}.

Let us follow some selected instructions characteristic of the AutoLISP language of programming the AutoCAD graphic editor used in the novel application to create the investigated reference networks. The procedure presented in Line 1 instructs the displacement of a local coordinate system to the position of the global coordinate system $[x,y,z]$. Line 2 contains the instruction giving the W_{AB12} point coordinates identical to the coordinates of the point W_{CD11}. Instructions of Lines 3 and 4 calculate the coordinates of the points W_{AD12} and W_{BC12} on the side edges $b_{12} = c_{11}(W_{CD11},W_{BC11})$ and $a_{12} = d_{11}(W_{CD11},W_{AD11})$ by means of two division coefficients—dWBC12 and dWAD12—of the pairs (W_{CD11},W_{BC11}) and (W_{CD11},W_{AD11}) by W_{BC12} and W_{AD12}.

```
Line 1: (command "luw" "g")
Line 2: (setq WAB12 (cal "WCD11+Oo"))
Line 3: (setq WBC12 (cal "plt(WCD11,WBC11,dWBC12)"))
Line 4: (setq WAD12 (cal "plt(WCD11,WAD11,dWAD12)"))
Line 5: (setq O12 (cal "plt(WBC12,WAD12,0.5)"))
Line 6: (command "luw" "3" WBC12 WAD12 WAB12)
Line 7: (setq O12u (cal "w2u(O12)"))
Line 8: (command "luw" "_o" O12u)
Line 9: (command "luw" "x" alfCD12)
Line 10: (setq WCD12u (list 0.0 jcd12 0.0) WCD12 (cal "u2w(WCD12u)"))
```

By means of the instruction from Line 6, a local clockwise coordinate system $[x_L,y_L,z_L]$ with the origin at W_{BC12} is created so that the positive half axis x_L is determined by the points W_{BC12} and W_{AD12}, and the positive half axis y_L is contained in the plane $(W_{BC12},W_{AD12},W_{AB12})$, where the point W_{AB12} determines its positive course. The axis z_L passes through W_{BC12} perpendicularly to the plane (x_L,y_L), so that, the system $[x_L,y_L,z_L]$ is clockwise. Then, $[x_L,y_L,z_L]$ is moved into a new position $[x_{L1},y_{L1},z_{L1}]$ according to the instruction assigned to Line 8. After executing this instruction, the origin of $[x_{L1},y_{L1},z_{L1}]$ is located in the middle point O_{12} of $W_{BC12}W_{AD12}$ (Figure 9b).

Since the translation of the old system $[x_L,y_L,z_L]$ to its new position $[x_{L1},y_{L1},z_{L1}]$ has to be performed, the coordinates of the point O_{12} must be transformed into the new system. This action is initiated by the procedure shown in Line 7. The instruction given in Line 9 rotates the system $[x_{L1},y_{L1},z_{L1}]$ to its new position $[x_{L2},y_{L2},z_{L2}]$. The point W_{CD12u} takes the coordinates (0.0 jcd12 0.0) in its new position, according to the instruction given in Line

10. The height of the triangle $W_{AB12}W_{BC12}W_{AD12}$, passed from the point W_{AB12} is equal to jcd12. In the second part of Line 10, the coordinates of W_{CD12} are transformed from the local system $[x_{L2}, y_{L2}, z_{L2}]$ to the global system $[x, y, z]$.

The code of the presented application contains two main instructions (while...) for creating subsequent meshes Γ_{ij} located in two orthogonal directions, that is, in *i* rows and *j* columns of the network Γ. The selection function (cond...) makes it possible to distinguish and determine four sets of these meshes. The first set relates to the first mesh Γ_{11}. The subsequent two sets concern the meshes located in two orthogonal directions passing along the planes (x, z) and (y, z). The last set of meshes is related to the diagonal directions relative to Γ_{11}.

```
(setq i 0)

(while (<= i iN)

(setq j 0)

(setq i (+ i 1))

(while (<= j jN)

(setq j (+ j 1))

    (cond ((and (= i 1) (= j 1))      (progn ... creation of the first Γ₁₁))

          ((and (= i 1) (> j 1))      (progn ... creation of the first type of orthogonal reference

                                       tetrahedrons Γ₁ⱼ))
          ((and (> i 1) (= j 1))      (prong ... creation of the second type of orthogonal reference

                                       tetrahedrons Γᵢ₁))
          ((and (> i 1) (> j 1))      (progn ... creation of diagonal reference tetrahedrons Γᵢⱼ)

    );cond

);while.

);while
```

The above-mentioned procedures are represented by the block scheme shown in Figure 11. They are the main part of the method's algorithm presented in this article.

To determine four points S_{A11}, S_{B11}, S_{C11} and S_{D11} (Figure 12a) defining a sector of a reference surface, four division coefficients constituting four elements of the first set of the initial data must be employed. Subsequently, four auxiliary points of the reference surface must be determined on the side edges of Γ_{12} so that two of them $S_{B12} = S_{C11}$, $S_{A12} = S_{D11}$ belong to $b_{12} = c_{11}$ and $a_{12} = d_{11}$, and the other two—S_{C12} and S_{D12}—are determined on two side edges c_{12} and d_{12} using two division coefficients constituting two elements of the second set of the initial data adopted earlier (Figure 12b). Tetrads of points S_{A1j}, S_{B1j}, S_{C1j} and S_{D1j} belonging to the remaining tetrahedrons Γ_{1j} (for $j > 2$) arranged along the (x, z)-plane are determined in an analogous manner.

At the subsequent step of the method's algorithm, four auxiliary points S_{A21}, S_{B21}, S_{C21} and S_{D21} of the reference surface must be determined on the side edges of Γ_{21}, so that two of them are $S_{A21} = S_{B11}$, $S_{D21} = S_{C11}$, and the other two S_{C21} and S_{B21} are determined on two side edges c_{21} and b_{21} (Figure 13), using two division coefficients of the third set of the initial data.
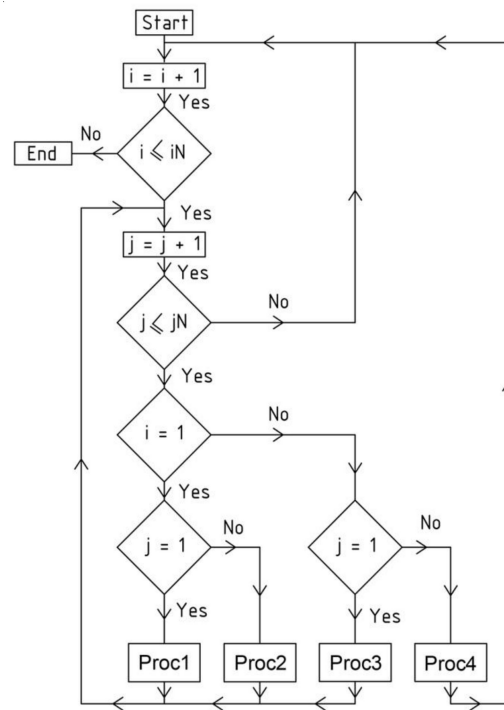
Figure 11. The algorithm of the iterative process for creating the nets Γ and B_v and structures Ω and $\sum$.

(**a**)

(**b**)
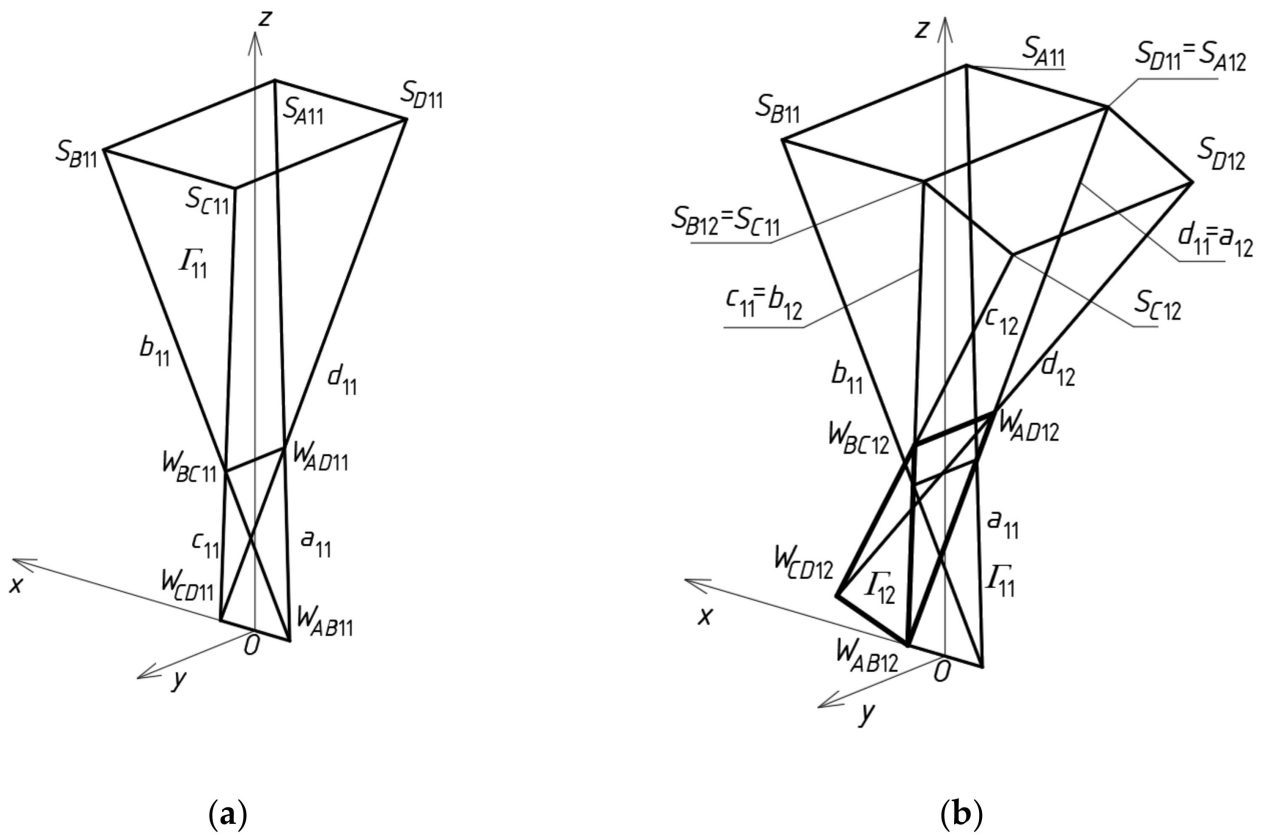
Figure 12. Tetrads of the ω_r's points belonging to: (**a**) Γ_{11}; (**b**) Γ_{12}.
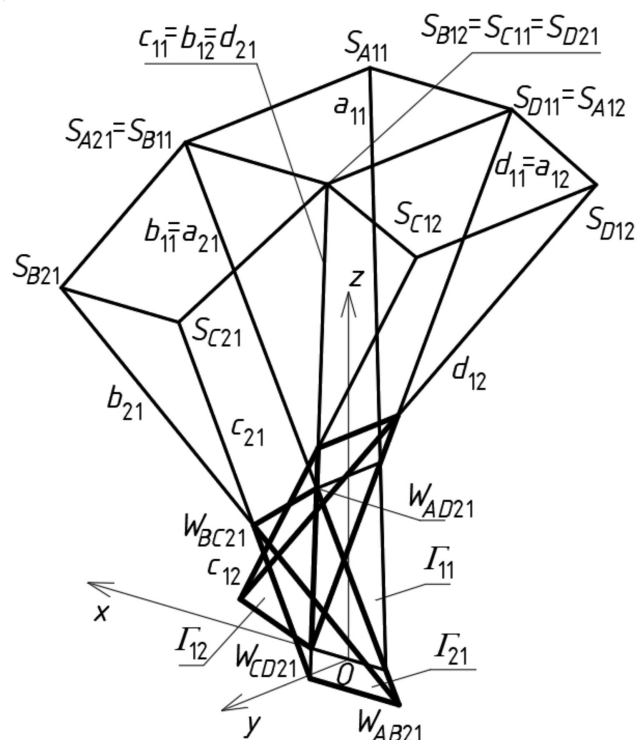
Figure 13. Subsequent tetrads of the points belonging to Γ_{21}.

At the end of this step, four auxiliary points f the ω_r reference surface are determined on the side edges of Γ_{22}. Three of these points are determined on $a_{22} = b_{12}$, $b_{22} = c_{21}$, and $d_{22} = c_{12}$, so that $S_{A22} = S_{B12}$, $S_{B22} = S_{C21}$ and $S_{D22} = S_{C12}$ (Figure 14). The last one belongs to c_{22} determined by W_{CD22} and W_{BC22}, using a division coefficient constituting one element of the fourth set of the initial data.
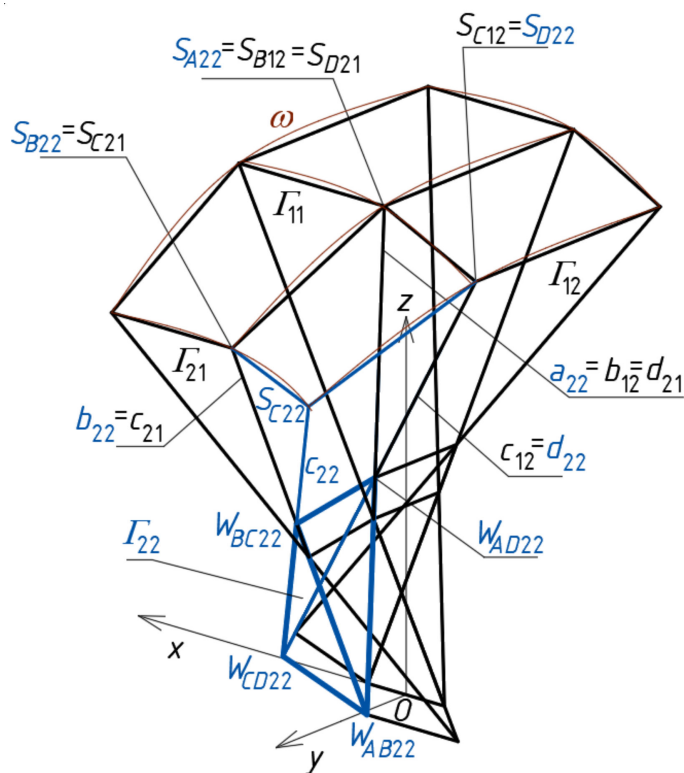
Figure 14. An auxiliary quadrilateral net determining a reference surface ω the polyhedral net Γ.

Tetrads of points S_{Aij}, S_{Bij}, S_{Cij} and S_{Dij} belonging to the remaining tetrahedrons Γ_{ij} (for $i,j > 2$) arranged diagonally in relation to Γ_{11} have to be determined in an analogous manner. On the basis of the auxiliary quadrilateral net having vertices located at the points S_{Aij}, S_{Bij}, S_{Cij} and S_{Dij} of Γ_{ij}, the ω_r surface is defined (Figure 14).

Some procedures related to the determination of the aforementioned points S_{Aij}, S_{Bij}, S_{Cij} and S_{Dij} are presented and analyzed below. The procedures shown in Lines 11 to 14 realize the calculations of the coordinates of the above points. The procedure given in Line 15 creates the plane quadrangle $S_{A11}S_{B11}S_{C11}S_{D11}$ in the three-dimensional computer space.

Line 11: (setq SA11 (cal "plt(WAB11,WAD11,dSA11)"))
Line 12: (setq SB11 (cal "plt(WAB11,WBC11,dSB11)"))
Line 13: (setq SD11 (cal "plt(WCD11,WAD11,dSD11)"))
Line 14: (setq SC11 (cal "plt(WCD11,WBC11,dSC11)"))
Line 15: (command "linia" SA11 SB11 SC11 SD11 SA11 "")

The instructions assigning the values of the coordinates of the previously determined points S_{D11} and S_{C11} to the coordinates of S_{A12} and S_{B12} are presented in Lines 16 and 17. The procedure from Line 18 calculates the division coefficient of the pair (W_{AB12},W_{AD12}) by S_{A12} using an internal novel function (wspolcz...) written by the author. The next instruction located in Line 19 assigns the value calculated by the function (wspolcz...) to the division coefficient dSA12.

The analogous procedures resulting in the calculation of the coefficient dSB12 of the pair (W_{AB12},W_{BC12}) by S_{B12} are given in Lines 20 and 21. The instructions from Lines 22 and 23 calculate the coordinates of the points S_{C12} and S_{D12} positioned on the straight lines (W_{CD12},W_{BC12}) and (W_{CD12},W_{AD12}), using the division coefficients dWBC12 and dWAD12 of the aforementioned pairs by S_{C12} and S_{D12}. The procedure shown in Line 24 creates a quadrangle $S_{A12}S_{B12}S_{C12}\,S_{D12}$ in the three-dimensional computer space.

Line 16: (setq SA12 (cal "SD11 + Oo"))
Line 17: (setq SB12 (cal "SC11 + Oo"))
Line 18: (wspolcz SA12 WAB12 WAD12)
Line 19: (setq dSA12 wspcz)
Line 20: (wspolcz SB12 WAB12 WBC12)
Line 21: (setq dSB12 wspcz)
Line 22: (setq SC12 (cal "plt(WCD12,WBC12,dSC12)"))
Line 23: (setq SD12 (cal "plt(WCD12,WAD12,dSD12)"))
Line 24: (command "linia" SA12 SB12 SC12 SD12 SA12 "")

The procedures calculating the coordinates of S_{A22}, S_{B22}, S_{C22} and S_{D22} are analogous to those presented earlier for Γ_{11} and Γ_{12}. The internal function (wspolcz...) must be used three times to calculate the coordinates of the above three points. In the case of Γ_{22}, the value of the calculated division coefficient dSA22 of (W_{AB22},W_{AD22}) by S_{C11} have to be assigned to the division coefficient dSC22 of (W_{CD22},W_{BC22}) by S_{C2}.

It is worth paying attention to the following properties of the reference network Γ built so far. All vertices of each reference tetrahedron Γ_{ij} designate four side edges a_{ij}, b_{ij}, c_{ij} and d_{ij} and four planes of Γ. Each new reference tetrahedron Γ_{i+1j} or Γ_{ij+1} is created as a spatial mesh with two sought-after vertices defined on two side edges of two previously constructed tetrahedrons Γ_{ij}, so the subsequent pairs of adjacent meshes of Γ have to have common planes. The roof directrices of each Γ_{ij} should be positioned in these planes.

To calculate the coordinates of A_{11}, B_{11}, C_{11} and D_{11} of a closed spatial eaves quadrangle B_{v11}, four division coefficients constituting four elements of the first set of the initial data, used for Γ_{11}, have to be adopted. These points belong to four side edges $a_{11}(W_{AB11},W_{AD11})$, $b_{11}(W_{AB11},W_{BC11})$, $c_{11}(W_{BC11},W_{CD11})$ and $d_{11}(W_{CD11},W_{AD11})$ and should be positioned in accordance with ω_r by means of the respective division coefficients (Figure 15a). Subsequently, four vertices—A_{12}, B_{12}, C_{12} and D_{12} of B_{v12}—have to be determined on the side edges a_{12}, b_{12}, c_{12} and d_{12} of Γ_{12} in relation to ω_r. Two of these vertices

are $A_{12} = C_{11}$, $B_{12} = D_{11}$. The other two C_{12} and D_{12} have to be determined on two side edges $c_{12}(W_{BC12}, W_{CD12})$ and $d_{12}(W_{CD12}, W_{AD12})$ using two division coefficients constituting two elements of the second set of the initial data. The tetrads of points A_{1j}, B_{1j}, C_{1j} and D_{1j} belonging to the side edges of the remaining tetrahedrons Γ_{1j} (for $j > 2$) and constituting the vertices of the remaining spatial quadrangles B_{v1j} located along the (x,z)-plane are determined in an analogous manner.
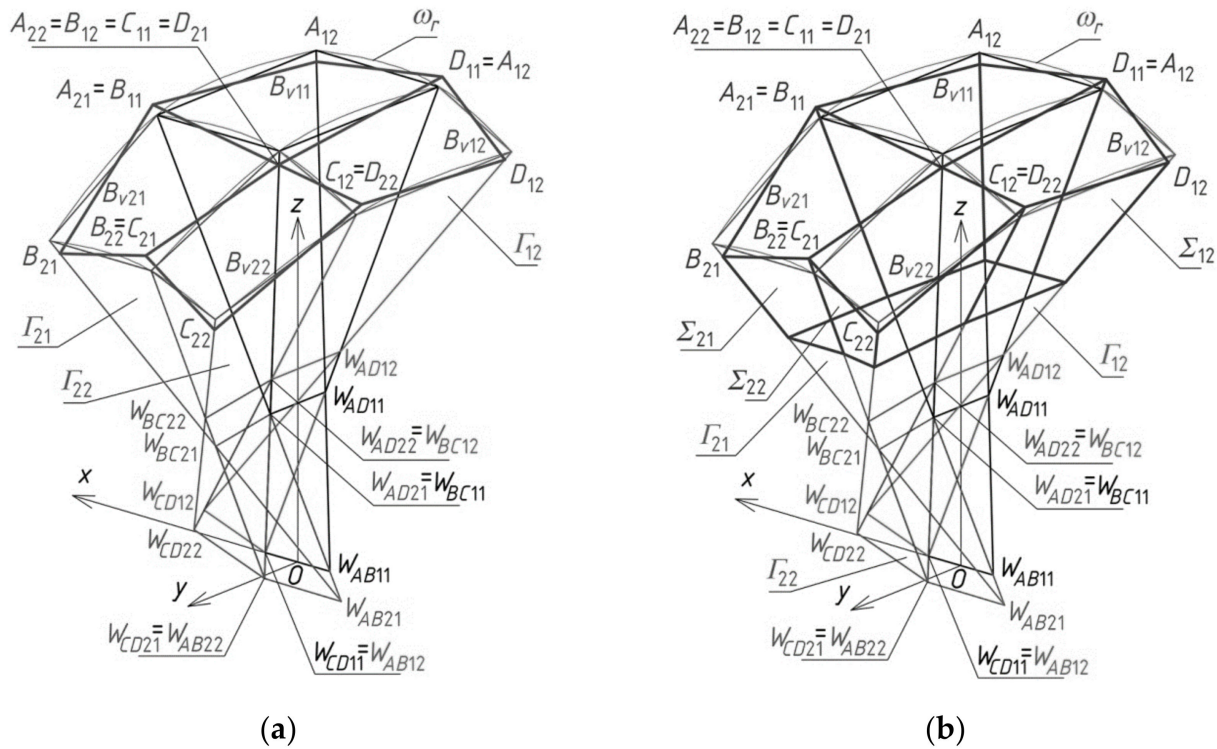

Figure 15. Final steps of creating: (**a**) B_v net; (**b**) elevation structure $\sum$.

Four vertices A_{21}, B_{21}, C_{21} and D_{21} of the eaves B_{v21} have to be determined on the side edges a_{21}, b_{21}, c_{21} and d_{21} of Γ_{21} in accordance with ω_r (Figure 15a). Two of these vertices are $A_{21} = B_{11}$, $D_{21} = C_{11}$. The other two C_{21} and B_{21} have to be determined on two side edges c_{21} (W_{BC21}, W_{CD21}) and $b_{21}(W_{AB21}, W_{BC21})$, using two division coefficients constituting two elements of the third set of the initial data. The points A_{i1}, B_{i1}, C_{i1} and D_{i1} belonging to the other tetrahedrons Γ_{i1} and constituting the vertices of the spatial quadrangles B_{vi1} (for $i > 2$) arranged along the (y,z)-plane are determined in an analogous manner.

Four vertices A_{22}, B_{22}, C_{22} and D_{22} of the quadrangle B_{v22} have to be determined on the side edges $a_{22}(W_{AB22}, W_{AD22})$, $b_{22}(W_{AB22}, W_{BC22})$, $c_{22}(W_{BC22}, W_{CD22})$ and $d_{22}(W_{CD22}, W_{AD22})$ of Γ_{22} relative to ω_r (Figure 15a). Three of these points are determined on $a_{22} = c_{11}$, $b_{22} = c_{21}$, and $d_{22} = c_{12}$ so that $A_{22} = C_{11}$, $B_{22} = C_{21}$ and $D_{22} = C_{12}$. The last one C_{22} belongs to $c_{22}(W_{CD22}, W_{BC22})$. It is determined by means of one division coefficient constituting an element of the fourth set of the initial data. The tetrads of points A_{ij}, B_{ij}, C_{ij} and D_{ij} belonging to the remaining tetrahedrons Γ_{ij} (for $i, j > 2$) arranged diagonally with regard to Γ_{22} can be determined in an analogous manner.

In order to determine a horizontal plane base of the free form $\sum$, one its point, for example, P_{D12} has to be defined on d_{12} (Figure 15b). The value of the division coefficient of the pair (W_{CD12}, W_{AD12}) by this point is an element of the second set of the initial data. Another point of the plane base is the intersection of the horizontal base plane passing through P_{D12} with the subsequent tetrads of side edges of Γ_{11}, Γ_{12}, etc.

The result of adding up the four reference tetrahedrons Γ_{ij} is a subnet Γ_1 constituting a quarter of the resultant reference network Γ. The other three parts of Γ can be built using

a *z*-axis symmetry and two (*x*,*z*)-plane and (*y*,*z*)-plane symmetries, called 3D-mirrors, in the way described in the next section on an example of a more complex reference network.

Similarly, four tetrahedrons $\sum_{ij}$ create a subnet $\sum_1$ constituting one-fourth of the designed building free form $\sum$. Four eaves quadrangles B_{vij} create a subnet B_{v1} constituting one-fourth of the network B_v. On the basis of B_v, the roof structure Ω composed of many sectors Ω_{ij} is created.

In summary, for the case of creating reference tetrahedrons Γ_{1j} or Γ_{i1} (for $j > 2$ or $i > 2$ and i, j different from (1) located in two orthogonal directions of planes (*x*,*z*) and (*y*,*z*), one vertex of each of these tetrahedrons must be located outside the side edges of the already created subnet of Γ. The vertex determines a new plane of Γ passing through the already constructed axis of the designed tetrahedron. Two of its subsequent vertices ought to be determined on two side edges of the previously created subnet of Γ with the help of two division coefficients. The location of the fourth vertex is identical with one of the vertices of Γ constructed earlier. In the case of the diagonal directions of Γ_{11}, each new reference tetrahedron Γ_{ij} has two vertices identical to two previously constructed vertices of Γ. However, its new vertices have to be determined on two side edges of the previously created subnet of Γ by means of the respective division coefficients.

This way of constructing the subsequent reference tetrahedrons located in the orthogonal and diagonal courses of each reference network Γ is characterized by the fact that each inner side edge of Γ is shared by four adjacent reference tetrahedrons and eight vertices of these four tetrahedrons belong to the same side edge of Γ. In a general case, these eight vertices occupy four different positions, in pairs. This topic is going to be presented in further publications. The example of using the proposed algorithm for determining the parametric reference polyhedral networks Γ and eaves nets B_v is given in next section.

6. Results—Parametric Shaping of the Reference Networks

Two ways of shaping of the investigated networks Γ and B_v can be carried out in scientific and engineering problems. One of these ways is based on the stiff-motions such as translations and rotations of several initially adopted or calculated points edges and planes determining the other vertices and side edges of these nets [22]. The second way, presented in this article, is more intuitive, because it enables one to create parametric models by means of the division coefficients expressing very specific relations between the main elements of the designed building free-forms. To make this method easy for many designers, a novel computer application written in the AutoLISP language of programming the AutoCAD visual editor was developed.

The last way requires a little more operations related to the division coefficients of the respective pairs of the determined vertices of the investigated reference polyhedral Γ and the quadrilateral B_v networks. The coefficients define the positions of: (1) the vertices of the sought-after reference network Γ with respect to a few intuitively adopted specific points of Γ, (2) the planes of Γ, (3) the points S_{Aij}, S_{Bij}, S_{Cij}, and S_{Dij} belonging to ω_r, and (4) the vertices A_{ij} B_{ij}, C_{ij} and D_{ij} of B_v determining the multi-shell roof structure Ω.

In the example presented below, a usage of the method for computational determining one quarter Γ_1 of a reference network Γ (Figure 16) based on some adopted proportions is discussed. All vertices of three other quarters Γ_{2L}, Γ_{3p}, Γ_{4r} of Γ are determined using: (1) *z*-axial symmetry for the case of Γ_{2L}, (2) (*x*,*z*)-plane symmetry called 3D-mirror for Γ_{3p}, and (3) (*y*,*z*)-plane symmetry for the case of Γ_{4r}. A description of creating the symmetric nets Γ_{2L}, Γ_{3p}, Γ_{4r} is not presented in this article.

Creating one quarter Γ_1 of an *z*-axially symmetric network Γ is started by defining the first *z*-axis-symmetric mesh Γ_{11} (Figure 17a). It is continued for subsequent meshes Γ_{ij} arranged orthogonally (Figure 17b) and, next, diagonally with respect to Γ_{11}, following the algorithm presented in the previous section. To obtain the first tetrahedron Γ_{11}, four of its vertices—W_{AB11}, W_{CD11}, W_{AD11} and W_{BC11}—are defined by means of their coordinates listed in Table 1.

Figure 16. A multi-segment reference network Γ consisting of four symmetric subnets Γ_1, Γ_{2L}, Γ_{3p} and Γ_{4r}.

(**a**)   (**b**)   (**c**)
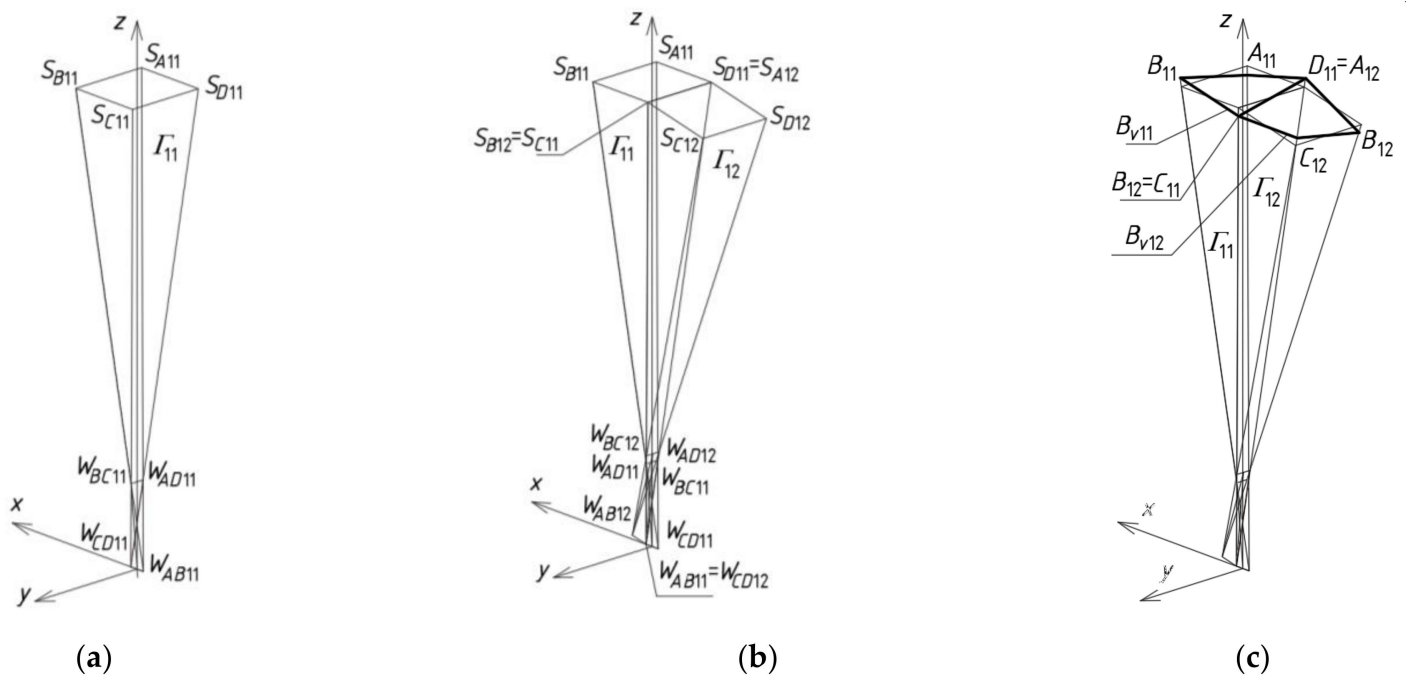
Figure 17. Two initial steps of the method's algorithm related to creation of: (**a**) Γ_{11}; (**b**) Γ_{12}; (**c**) B_{v11} and B_{v12}.

Table 1. The coordinates of Γ_{11}'s vertices.

Point	x-Coordinate (mm)	y-Coordinate (mm)	z-Coordinate (mm)
W_{AB11}	−1000	0	0
W_{CD11}	1000	0	0
W_{AD11}	0	−871.6	9961.90
W_{BC11}	0	871.6	9961.90

The positions of the points S_{A11}, S_{B11}, S_{C11} and S_{D11} of ω_r are defined with the following division coefficients $(W_{AB11}, W_{AD11})\backslash S_{A11}$, $(W_{AB11}, W_{BC11})\backslash S_{B11}$, $(W_{CD11}, W_{BC11})\backslash S_{C11}$ and $(W_{CD11}, W_{AD11})\backslash S_{D11}$, where

$$(W_{AB11}, W_{AD11})\backslash S_{A11} = m(\overrightarrow{W_{AB11} S_{A11}})/m(\overrightarrow{W_{AB11} W_{AD11}})$$
$$(W_{AB11}, W_{BC11})\backslash S_{B11} = m(\overrightarrow{W_{AB11} S_{B11}})/m(\overrightarrow{W_{AB11} W_{BC11}})$$
$$(W_{CD11}, W_{BC11})\backslash S_{C11} = m(\overrightarrow{W_{CD11} S_{C11}})/m(\overrightarrow{W_{CD11} W_{BC11}})$$
$$(W_{CD11}, W_{AD11})\backslash S_{D11} = m(\overrightarrow{W_{CD11} S_{D11}})/m(\overrightarrow{W_{CD11} W_{AD11}})$$

and $\overrightarrow{W_{AB11} W_{AD11}}$ is the vector starting with W_{AB11} and ending at W_{AD11}, $m(\overrightarrow{W_{AB11} W_{AD11}})$ is the measure of $\overrightarrow{W_{AB11} W_{AD11}}$, $\overrightarrow{W_{AB11} S_{A11}}$ is the vector with the starting point at W_{AB11} and the ending point at S_{A11}, etc. The values of the above ratios are listed in Table 2. The subsequent points S_{A11}, S_{B11}, S_{C11} and S_{D11} define the spatial quadrangle determining a respective segment of ω_r.

Table 2. The initial data defining the meshes Γ_{11} and B_{v11}.

Division Coefficient	Value
$(W_{AB11}, W_{AD11})\backslash S_{A11}$	5.5
$(W_{AB11}, W_{BC11})\backslash S_{B11}$	5.5
$(W_{CD11}, W_{AD11})\backslash S_{C11}$	5.5
$(W_{CD11}, W_{AD11})\backslash S_{D11}$	5.5
$(W_{AB11}, W_{AD11})\backslash (S_{A11}, A_{11})$	-0.1
$(W_{AB11}, W_{BC11})\backslash (S_{B11}, B_{11})$	0.1
$(W_{CD11}, W_{BC11})\backslash (S_{C11}, C_{11})$	-0.1
$(W_{CD11}, W_{AD11})\backslash (S_{D11}, D_{11})$	0.1

The locations of the vertices A_{11}, B_{11}, C_{11} and D_{11} of Γ_{11} (Figure 17c) are defined by means of the aforementioned vertices of Γ_{11} and the following proportions

$$(W_{AB11}, W_{AD11})\backslash A_{11} = m(\overrightarrow{W_{AB11} A_{11}})/m(\overrightarrow{W_{AB11} W_{AD11}})$$
$$(W_{AB11}, W_{BC11})\backslash B_{11} = m(\overrightarrow{W_{AB11} B_{11}})/m(\overrightarrow{W_{AB11} W_{BC11}})$$
$$(W_{CD11}, W_{BC11})\backslash C_{11} = m(\overrightarrow{W_{CD11} C_{11}})/m(\overrightarrow{W_{CD11} W_{BC11}})$$
$$(W_{CD11}, W_{AD11})\backslash D_{11} = m(\overrightarrow{W_{CD11} D_{11}})/m(\overrightarrow{W_{CD11} W_{AD11}})$$

where $\overrightarrow{W_{AB11} A_{11}}$ is the vector defined by the starting point at W_{AB11} and the ending point A_{11}, etc. The points A_{11}, B_{11}, C_{11} and D_{11} determine the spatial quadrangle B_{v11} limiting the single smooth shell segment Ω_{11} of the complex roof structure Ω. Subsequently, the values of four division coefficients $(W_{AB11}, W_{AD11})\backslash (S_{A11}, A_{11})$, $(W_{AB11}, W_{BC11})\backslash (S_{B11}, B_{11})$, $(W_{CD11}, W_{BC11})\backslash (S_{C11}, C_{11})$ and $(W_{CD11}, W_{AD11})\backslash (S_{D11}, D_{11})$ must be adopted as follows

$$(W_{AB11}, W_{AD11})\backslash (S_{A11}, A_{11}) = m(\overrightarrow{S_{A11} A_{11}})/m(\overrightarrow{W_{AB11} W_{AD11}}) = (W_{AB11}, W_{AD11})\backslash A_{11} \text{-} (W_{AB11}, W_{AD11})\backslash S_{A11}$$
$$(W_{AB11}, W_{BC11})\backslash (S_{B11}, B_{11}) = m(\overrightarrow{S_{B11} B_{11}})/m(\overrightarrow{W_{AB11} W_{BC11}}) = (W_{AB11}, W_{BC11})\backslash B_{11} \text{-} (W_{AB11}, W_{BC11})\backslash S_{B11}$$
$$(W_{CD11}, W_{BC11})\backslash (S_{C11}, C_{11}) = m(\overrightarrow{S_{C11} C_{11}})/m(\overrightarrow{W_{CD11} W_{BC11}}) = (W_{CD11}, W_{BC11})\backslash C_{11} \text{-} (W_{CD11}, W_{BC11})\backslash S_{C11}$$
$$(W_{CD11}, W_{AD11})\backslash (S_{D11}, D_{11}) = m(\overrightarrow{S_{D11} D_{11}})/m(\overrightarrow{W_{CD11} W_{AD11}}) = (W_{CD11}, W_{AD11})\backslash D_{11} \text{-} (W_{CD11}, W_{AD11})\backslash S_{D11}$$

The above constants have positive or negative signs depending on whether the points A_{11}, B_{11}, C_{11} and D_{11} lie above or below ω_r defined by means of the quadrangle $S_{A11} S_{B11} S_{C11} S_{D11}$ (Figure 17a).

If we transform the above formulas, the division ratios $(W_{AB11}, W_{AD11})\backslash A_{11}$, $(W_{AB11}, W_{BC11})\backslash B_{11}$, $(W_{CD11}, W_{BC11})\backslash C_{11}$ and $(W_{CD11}, W_{AD11})\backslash D_{11}$ can be calculated as follows

$$(W_{AB11}, W_{AD11})\backslash A_{11} = (W_{AB11}, W_{AD11})\backslash S_{A11} + (W_{AB11}, W_{AD11})\backslash (S_{A11}, A_{11})$$
$$(W_{AB11}, W_{BC11})\backslash B_{11} = (W_{AB11}, W_{BC11})\backslash S_{B11} + (W_{AB11}, W_{BC11})\backslash (S_{B11}, B_{11})$$
$$(W_{CD11}, W_{BC11})\backslash C_{11} = (W_{CD11}, W_{BC11})\backslash S_{C11} + (W_{CD11}, W_{BC11})\backslash (S_{C11}, C_{11})$$
$$(W_{CD11}, W_{AD11})\backslash D_{11} = (W_{CD11}, W_{AD11})\backslash S_{D11} + (W_{CD11}, W_{AD11})\backslash (S_{D11}, D_{11})$$

The values of the division coefficients used in the example are given in Table 2.

In order to create the tetrahedron Γ_{12}, four of its vertices—W_{AB12}, W_{CD12}, W_{AD12} and W_{BC12}—were defined by means of the coordinates listed in Table 3.
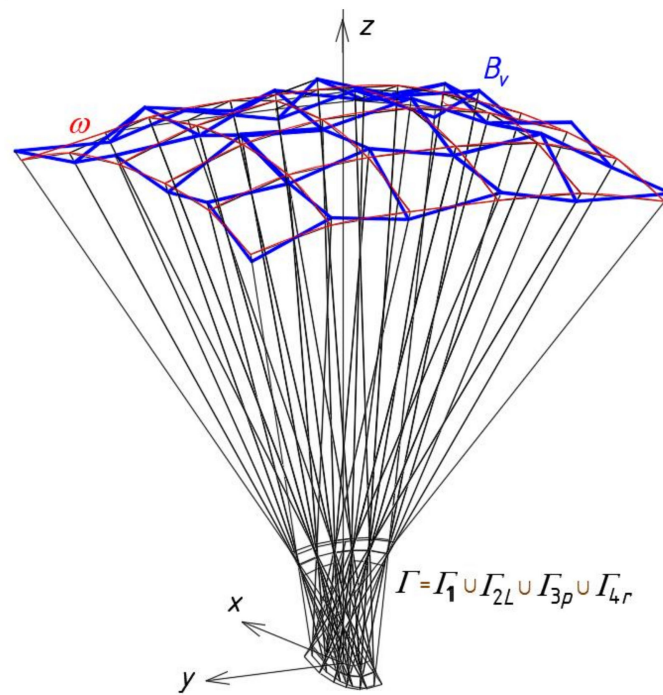
Table 3. The coordinates of the Γ_{12}'s vertices.

Point	x-Coordinate (mm)	y-Coordinate (mm)	z-Coordinate (mm)
W_{AB12}	4500.00	4880.70	55,786.90
W_{CD12}	3254.30	0	468.2
W_{AD12}	−100	−958.7	10,958.10
W_{BC12}	−100	958.7	10,958.10

The positions of the points S_{A12}, S_{B12}, A_{12} and B_{12} are similar to the positions of S_{D11}, S_{C11}, D_{11} and C_{11}, so the following division coefficients have to be calculated as follows

$(W_{AB12}, W_{AD12}) \backslash S_{A12} = (W_{CD11}, W_{AD11}) \backslash S_{D11} / (W_{CD11}, W_{AD11}) \backslash W_{AD12}$

$(W_{AB12}, W_{BC12}) \backslash S_{B12} = (W_{CD11}, W_{BC11}) \backslash S_{C11} / (W_{CD11}, W_{BC11}) \backslash W_{BC12}$

$(W_{AB12}, W_{AD12}) \backslash A_{12} = (W_{CD11}, W_{AD11}) \backslash D_{11} / (W_{CD11}, W_{AD11}) \backslash W_{AD12}$

$(W_{AB12}, W_{BC12}) \backslash B_{12} = (W_{CD11}, W_{BC11}) \backslash C_{11} / (W_{CD11}, W_{BC11}) \backslash W_{BC12}$

where the spaces before and behind the slash denote that we have common division of two numbers. Other division ratios related to Γ_{12} and B_{v12} are adopted as follows.

(WCD12,WBC12)\SC12 = (WAB12,WAD12)\SA12

(WCD12,WAD12)\SD12 = (WAB12,WBC12)\SB12

(WCD12,WBC12)\C12 = (WAB12,WAD12)\A12

(WCD12,WAD12)\D12 = (WAB12,WBC12)\B12

The calculated values of these division coefficients are given in Table 4.

Table 4. The data defining the mesh B_{v12}.

Ratio	Value
$(W_{AB12}, W_{AD12}) \backslash S_{A12}$	5
$(W_{AB12}, W_{BC12}) \backslash S_{B12}$	5
$(W_{CD12}, W_{BC12}) \backslash S_{C12}$	5
$(W_{CD12}, W_{AD12}) \backslash S_{D12}$	5
$(W_{AB12}, W_{AD12}) \backslash (S_{A12}, A_{12})$	0.091
$(W_{AB12}, W_{BC12}) \backslash (S_{A12}, B_{12})$	−0.091
$(W_{CD12}, W_{BC12}) \backslash (S_{A12}, C_{12})$	0.091
$(W_{CD12}, W_{AD12}) \backslash (S_{A12}, D_{12})$	−0.091

The positions of the points: (1) S_{A13}, S_{B13}, S_{C13}, S_{D13}, A_{13}, B_{13}, C_{13} and D_{13}, (2) S_{A21}, S_{B21}, S_{C21}, S_{D21}, A_{21}, B_{21}, C_{21} and D_{21}, (3) S_{A31}, S_{B31}, S_{C31}, S_{D31}, A_{31}, B_{31}, C_{31} and D_{31} can be defined or calculated in an analogous way, as for S_{A12}, S_{B12}, S_{C12}, S_{D12}, A_{12}, B_{12}, C_{12} and D_{12}. The values of the coordinates of all aforementioned points are given in Tables A2 and A3, posted in Appendix A.

To determine the last tetrahedron Γ_{22} investigated in our example, four of its vertices—W_{AB22}, W_{CD22}, W_{AD22} and W_{BC22} (Figure 18)—are initially defined by means of the coordinates listed in Table 5.

Table 5. The coordinates of the Γ_{22}'s vertices.

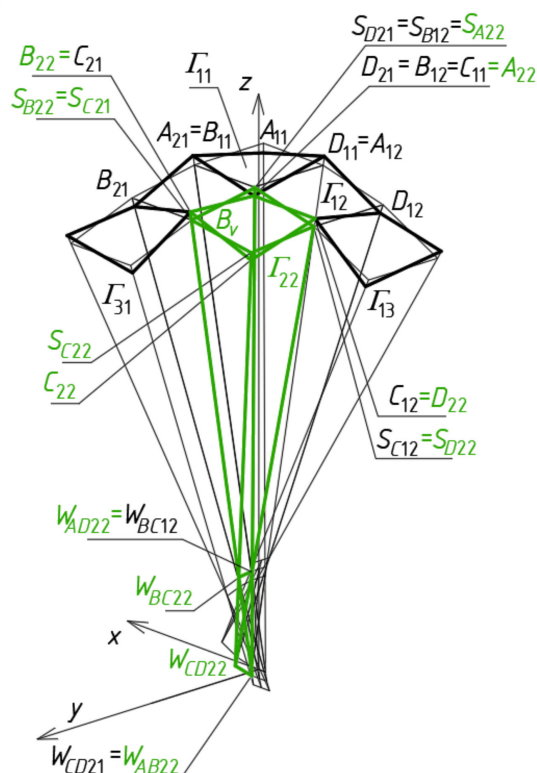| Point	x-Coordinate (mm)	y-Coordinate (mm)	z-Coordinate (mm)
W_{AB22}	1100.00	−87.2	−996.2
W_{CD22}	3589.70	−95.9	−580.8
W_{AD22}	−100	958.7	10,958.10
W_{BC22}	−110	2840.10	10,744.40

Figure 18. The reference tetrahedron Γ_{22} and spatial quadrangle B_{v22}.

To construct the quadrangle B_{v22} (Figure 18), the values of the vertices S_{A22}, S_{B22}, S_{C22}, S_{D22}, A_{22}, B_{22}, C_{22} and D_{22} must be calculated in the following way. The positions of the points S_{A22}, S_{B22}, S_{D22}, A_{22}, B_{22} and D_{22} are similar to the positions of S_{C11}, S_{C21}, S_{C12}, C_{11}, C_{21} and C_{12} determined previously for Γ_{11}, Γ_{21}, Γ_{12}, B_{v11}, B_{v21} and B_{v12}.

To achieve the coordinates of the aforementioned points of ω_r and B_v, the following division coefficients should be calculated

$$(W_{AB22}, W_{AD22})\backslash S_{A22} = \frac{(WCD11, WBC11)\backslash SC11}{(WCD11, WBC11)\backslash WAD22 \cdot (WBC11, WCD11)\backslash WAB22}$$

$$(W_{AB22}, W_{AD22})\backslash A_{22} = \frac{(WCD11, WBC11)\backslash C11}{(WCD11, WBC11)\backslash WAD22 \cdot (WBC11, WCD11)\backslash WAB22}$$

$$(W_{AB22}, W_{AD22})\backslash (S_{A22}, A_{22}) = (W_{AB22}, W_{AD22})\backslash A_{22} - (W_{AB22}, W_{AD22})\backslash S_{A22}$$

$$(W_{AB22}, W_{BC22})\backslash S_{B22} = (W_{CD21}, W_{BC21})\backslash S_{C21} / (W_{CD21}, W_{BC21})\backslash W_{BC22}$$

$$(W_{AB22}, W_{BC22})\backslash B_{22} = (W_{CD21}, W_{BC21})\backslash C_{21} / (W_{CD21}, W_{BC21})\backslash W_{BC22}$$

$$(W_{AB22}, W_{BC22})\backslash (S_{B22}, B_{22}) = (W_{AB22}, W_{BC22})\backslash B_{22} - (W_{AB22}, W_{BC22})\backslash S_{B22}$$

$$(W_{CD22}, W_{AD22})\backslash S_{D22} = (W_{CD12}, W_{AD12})\backslash S_{C12} / (W_{BC12}, W_{CD12})\backslash W_{CD22}$$

$$(W_{CD22}, W_{AD22})\backslash D_{22} = (W_{CD12}, W_{AD12})\backslash C_{12} / (W_{BC12}, W_{CD12})\backslash W_{CD22}$$

$$(W_{CD22}, W_{AD22})\backslash (S_{D22}, D_{22}) = (W_{CD22}, W_{AD22})\backslash D_{22} - (W_{CD22}, W_{AD22})\backslash S_{D22}$$

A detailed description of a mutual position of the vertices belonging to one exemplary configuration of a polygonal B_v net and a polyhedral net Γ is presented by Abramczyk using the method based on stiff motions [22]. In the present article, the extensive method of parametric shaping of the regular roof shell structures by means of the orthotropic properties of the corrugated shell sectors is developed based on the division coefficients.

The spaces before and after slash/depict if a usual division is used. In contrast, a division ratio is expressed if there are not spaces before and after the backslash\. On the basis of the above division coefficients, the following can be calculated

$$(W_{CD22}, W_{BC22})\backslash S_{C22} = (W_{AB22}, W_{AD22})\backslash S_{A22}$$

$$(W_{CD22}, W_{BC22})\backslash C_{22} = (W_{AB22}, W_{AD22})\backslash A_{22}$$

$$(W_{CD22}, W_{BC22})\backslash (S_{C22}, C_{22}) = (W_{CD22}, W_{BC22})\backslash C_{22} - (W_{CD22}, W_{BC22})\backslash S_{C22}$$

The values of these division coefficients are given in Table 6.

Table 6. The initial data defining the mesh B_{v22}.

Ratio	Value
$(W_{AB22}, W_{AD22}) \backslash S_{A22}$	4.6667
$(W_{AB22}, W_{BC22}) \backslash S_{B22}$	4.6281
$(W_{CD22}, W_{AD22}) \backslash S_{D22}$	4.6667
$(W_{CD22}, W_{AD22}) \backslash S_{D22}$	4.6364
$(W_{AB22}, W_{AD22}) \backslash (S_{A21}, A_{22})$	-0.0833
$(W_{AB22}, W_{BC22}) \backslash (S_{A21}, B_{22})$	0.0826
$(W_{CD22}, W_{BC22}) \backslash (S_{A22}, C_{22})$	-0.0833
$(W_{CD22}, W_{AD22}) \backslash (S_{A22}, D_{22})$	0.0826

Analogous proportions as for the quadrangle Γ_{22} can be defined for other meshes located diagonally with respect to Γ_{11}, including for Γ_{23}, Γ_{32}, and Γ_{33}. The subnet Γ_1 constituting a sum of Γ_{ij} (for i,j = 1 to 3) is located between the planes (x,z) and (y,z) in the dihedral angle containing the positive axis y and the negative axis x (Figure 19). It is about one quarter of the designed resultant z-axis-symmetric Γ (Figure 16).
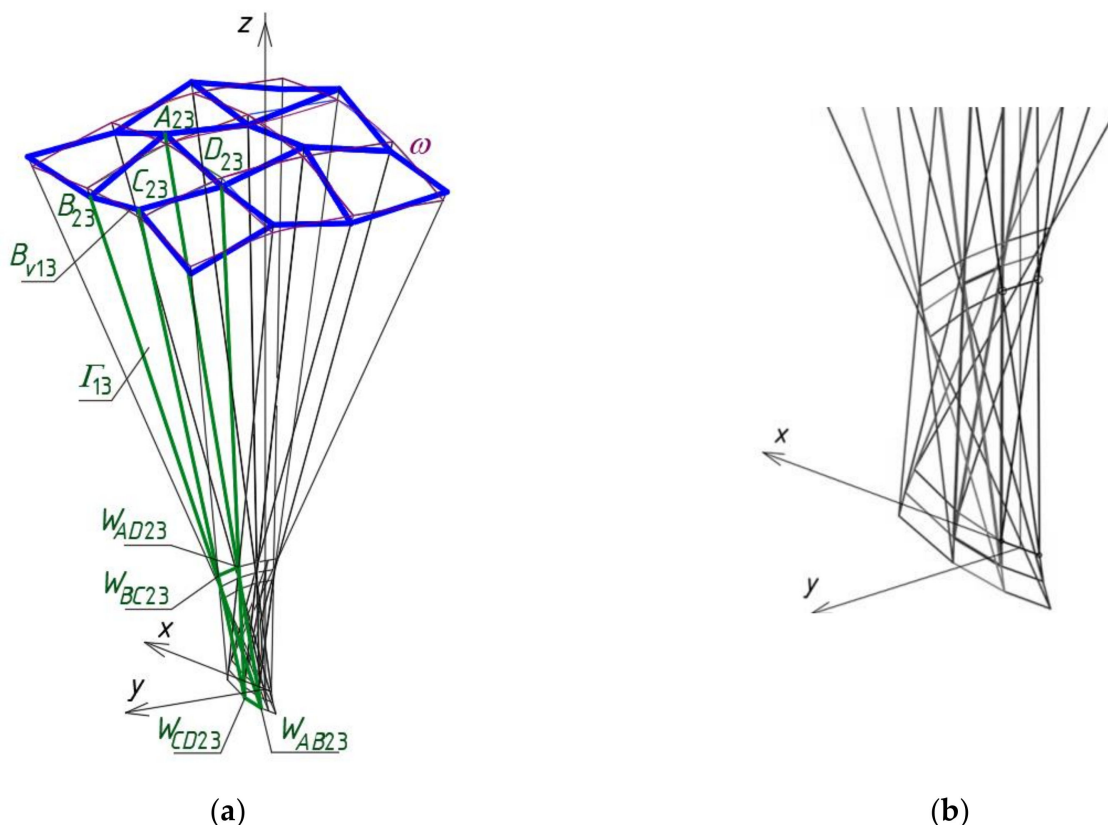
Figure 19. (**a**) The first quarter of the reference network Γ composed of Γ_{ij} for i,j = 1 to 3, (**b**) the Γ's vertices.

7. Discussion

The first basic goal accomplished by the proposed novel method is to create a relatively simple and regular spatial arrangement of many simple complete free forms connected to each other into one complex building free-form with oblique plane elevations and a transformed multi-segment shell roof structure. The individual free forms are roofed with single ruled shells whose shapes result from the expected shape transformations of thin-walled folded sheets. The simplicity of the method's algorithm is to build a system of planes that, when intersected, isolate many spatial meshes creating a reference network adaptable to various boundary conditions. These complete meshes also define the facade

walls of the designed complete free-forms. In these planes, common directrices of the shell segments roofing adjacent single free-forms are included. In the article, mutual skew straight lines are investigated as the roof directrices.

The regularity of numerous arrangements of many individual roof shell segments is ensured by the specific geometric shaping of these segments, based on the reference surface and division coefficients related to the intersecting point of respective planes and side edges of the reference networks. The most important steps of the method's algorithm leading to the achievement of the above assumed goal by means of a parameterization based on the aforementioned division coefficients are presented in Figures 11 and 20. The multitude and complexity of the activities and objects realized by the algorithm need to use computer technology to program the calculations and create the required geometric models.

Start

Assumptions:
- type of ω_r, the sign of the Gaussian curvature,
- type of Γ and its individual meshes Γ_{ij},
- the set of the selected single- and double-division ratios

Assumptions:
- type of B_v and its individual meshes B_{vij},
- the set of the selected single- and double-division ratios

Assumptions:
- type of W, where Wij on the basis of B_{vij},
- type of Σ, where Σ_{ij} on the basis of Γ_{ij},
- the set of the selected single- and double-division ratios

i = 00, iN, j = 0.0, jN

Performing an **iterative process** of calculating the vertives and creating the geometrical elements of:
- Γ a sum of Γ_{ij}, B_v a sum of B_{vij},
- Ω, a sum of Ω_{ij}, Σ a sum of Σ_{ij},

The obtained results set in four groups named Procedures:

Proc1 Proc2 Proc3 Proc4

Modifications:
- all elements of Γ_{ij}, B_{vij}, Σ_{ij}, Ω_{ij} to achieve their attractive forms or rational static-strength work
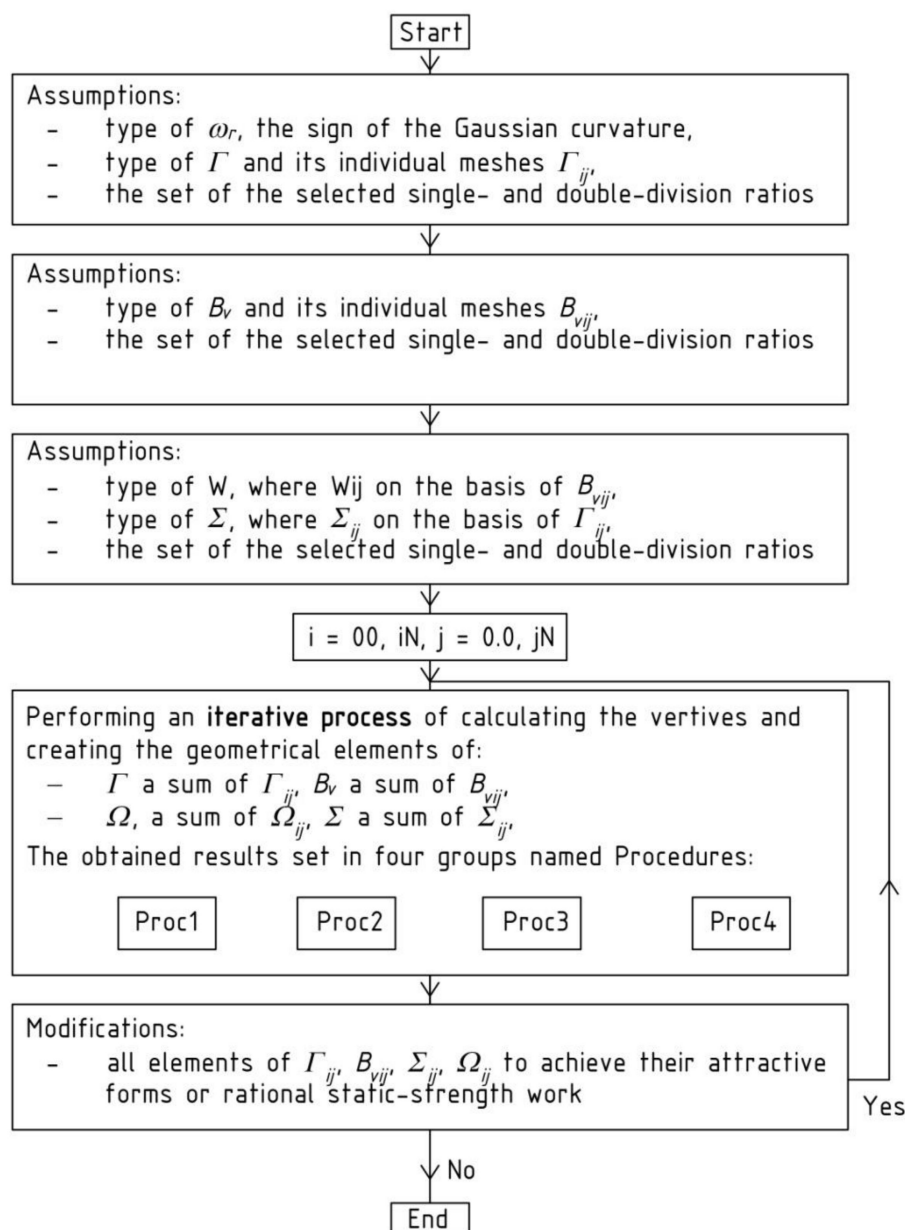
Yes

No

End

Figure 20. A block scheme of the method's algorithm.

The second main goal implemented by the method is the possibility of a relatively free and intuitive shaping of complex building free-form structures and their easy modification to the requirements and expectations of the designer.

To build a complex building form, the presented method's algorithm instructs the iterative activities and objects presented by means of the block scheme shown in Figure 11. At the beginning of each Γ's and B_v's shaping process, a set of numbers defining the locations of the vertices W_{ABij}, W_{CDij}, W_{ADij} and W_{BCij} of all subsequent reference tetrahedrons Γ_{ij} of Γ is adopted. The numbers are the division coefficients of the proper pairs of the already constructed vertices belonging to Γ_{ij} by the other sought-after vertices belonging to the subsequently determined tetrahedrons Γ_{i+1j}, Γ_{ij+1} and Γ_{i+1j+1}.

To create tetrahedrons Γ_{1j} and Γ_{i1} forming two principal orthogonal strips of Γ, a specific set of numbers constituting dependent or independent variables has to be adopted. To determine four vertices of each new reference tetrahedron located in one of these orthogonal strips, the following relations must be taken. Each tetrahedron has to have one common wall and two common side edges with one of the previously built reference tetrahedrons. Three other walls and two remaining side edges of this new reference tetrahedron are determined by means of two searched and two known vertices.

In order to determine the diagonal strips of the network Γ, a new set of parameters defining the location of four vertices of each tetrahedron Γ_{ij} located diagonally has to be adopted, so that: (1) two its walls and three side edges have to be common with some tetrahedrons constructed previously, and (2) one of these side edges must also be common with one of the previously constructed tetrahedrons of the same diagonal strip. Based on the above set, the locations of the remaining fourth side edge and two walls of this diagonal reference tetrahedron, for example Γ_{22}, are sought by means of two sought-after points belonging to two different side edges created previously.

Subsequently, the points S_{Aij}, S_{Bij}, S_{Cij} and S_{Dij} of a reference surface ω_r and the vertices of all B_{vij} meshes are determined on the basis of the reference network Γ and the adopted sets of initial data. These parameters are single-division coefficients and double-division coefficients of the subsequently selected pairs of the Γ's vertices by: (1) the points S_{Aij}, S_{Bij}, S_{Cij} and S_{Dij}, (2) the vertices A_{ij}, B_{ij}, C_{ij} and D_{ij} of B_{vij}, and (3) the points P_{Aij}, P_{Bij}, P_{Cij} and P_{Dij} of the base of the free-form-shaped building. In the example presented in the previous section, the calculated values of the division coefficients related to the positions of the aforementioned vertices are listed in Table 7.

Table 7. The division coefficients defining selected B_{vij}.

Ratio	Value
$(W_{AB11}, W_{AD11}) \backslash A_{11}$	5.4
$(W_{AB11}, W_{BC11}) \backslash B_{11}$	5.6
$(W_{CD11}, W_{BC11}) \backslash C_{11}$	5.4
$(W_{CD11}, W_{AD11}) \backslash D_{11}$	5.6
$(W_{AB12}, W_{AD12}) \backslash A_{12}$	5.091
$(W_{AB12}, W_{BC12}) \backslash B_{12}$	-4.909
$(W_{CD12}, W_{BC12}) \backslash C_{12}$	5.091
$(W_{CD12}, W_{AD12}) \backslash D_{12}$	-4.909
$(W_{AB22}, W_{AD22}) \backslash A_{22}$	4.5833
$(W_{AB22}, W_{BC22}) \backslash B_{22}$	4.7107
$(W_{CD22}, W_{BC22}) \backslash C_{22}$	4.5833
$(W_{CD22}, W_{AD22}) \backslash D_{22}$	4.7107

The main step of the method's algorithm is accomplished by means of the activities assigned to the sections Proc$k$, where $k = 1$ to 3 (Figure 20) depending on the location of Γ_{ij} in Γ. There are four configurations of these procedures, supporting the activities requiring different input data and various type and number of the functions used to determine the Γ's and B_v's vertices. The common actions assigned to all configurations are presented in the container called Procedure k shown in Figure 21. The activities are implemented in the innovative computer application written in the AutoLISP programming language.

Procedure *k*

(k = 1 for $i = j = 1$; k = 2 for i = 1 and j different from 1; k = 3 for j = 1 and i different from 1; k = 4 for i different from 1 and j different from 1):

- calculations of some single– and double division ratios, coordinates of all characteristic points and vertices,
- creating models of w_r, Γ_{ij}, Γ, B_{vij}, B_v, Ω_{ij}, Ω, Σ_{ij}, Σ

Figure 21. Common operations accomplished by the four configurations Prod*k*, where k = 1 to 4.

The actions of the section Proc1 (for k = 1) concern the first constructed meshes of networks Γ and B_v and the sectors of structures Ω and Σ, where $i = j = 1$. The activities referred to the section Proc2 (for k = 2), relating to the meshes of the first of two orthogonal strips of Γ, B_v, Ω and Σ running along the plane (x,z), for which i = 1 and j different from 1. The activities of the section Proc3 (for k = 3) relate to the meshes of the second orthogonal strip passing along the plane (y,z), for which j = 1 and i is different from 1. The activities assigned to the section Proc4 (for k = 4) refer to all meshes of the diagonal strips of Γ, B_v, Ω and Σ, for which i and j are different from 1. A novel computer-aided method is proposed due to the complexity of the above operations and geometric objects.

The division coefficients adopted initially to define the characteristic points of Γ, ω_r and B_v are also used for assessing the curvature of the reference surface ω_r and the roughness of the eaves net B_v. The expected curvature of the ω_r's area corresponding to the single mesh Γ_{ij} can be shaped by means of four division coefficients $(W_{ABij}, W_{ADij}) \backslash S_{Aij}$, $(W_{ABij}, W_{BCij}) \backslash S_{Bij}$, $(W_{CDij}, W_{BCij}) \backslash S_{Cij}$ and $(W_{CDij}, W_{ADij}) \backslash S_{Dij}$ determining the positions of the points S_{Aij}, S_{Bij}, S_{Cij} and S_{Dij} on the side edges a_{ij}, b_{ij}, c_{ij} and d_{ij}. Since the points are created for a finite number of subsequent meshes Γ_{ij}, then the curves located on ω_r can be defined in an approximate way on the basis of these points. These curves also define ω_r in an approximate way.

For the considered networks Γ and B_v and structures Ω and Σ, roughness of the B_v network also plays an important role. The roughness is determined by means of division coefficients of the respective pairs of the Γ's vertices by the selected ω_r's points and B_v's vertices. The roughness describes the disturbances in the smoothness of the network B_v in relation to the smooth surface ω_r. The disturbances result from the forced mutual inclination of each pair of the adjacent roof directrices designed for all complete meshes B_{vij} to realize the shape transformations of the complete corrugated roof shells. On the one hand, the roughness can have a positive effect on the attractiveness and span of the complex roof free forms Ω and entire building Σ. On the other hand, the edges between the adjacent meshes B_{vij} can reduce the visual attractiveness of the building shaped by disturbing the smoothness of the shell roof rib structure.

The maximum and minimum values of the absolute and relative roughness of the entire network B_v and the proportions between these values can be defined as double- and triple-division coefficients if the need exists. This problem also goes beyond the scope of the article.

The division coefficients of the selected pairs of the Γ_{ij}'s vertices by the points S_{Aij}, S_{Bij}, S_{Cij} and S_{Dij} affect the ω_r's curvature. If the values of the above coefficients are greater than 1, convex roof free forms with positive Gaussian curvatures are shaped (Figure 22a). If the values of the above coefficients are greater than 0 and less than 1, then concave roof shell forms with negative Gaussian curvature are shaped (Figure 22b). If the values of the above coefficients are from the range (-∞,0), concave roof free forms with positive Gaussian curvature are shaped. These forms have oblique facades tapering upwards in contrast to the forms widening upwards, e.g., the one presented in Figure 22a. A possibility of modifying the reference networks Γ by changing some division coefficients defining their

shapes and the positions of their vertices allows one to optimize the curvature of ω_r and the roughness of B_v according to the demands referring to the attractiveness of the shaped building free-forms.
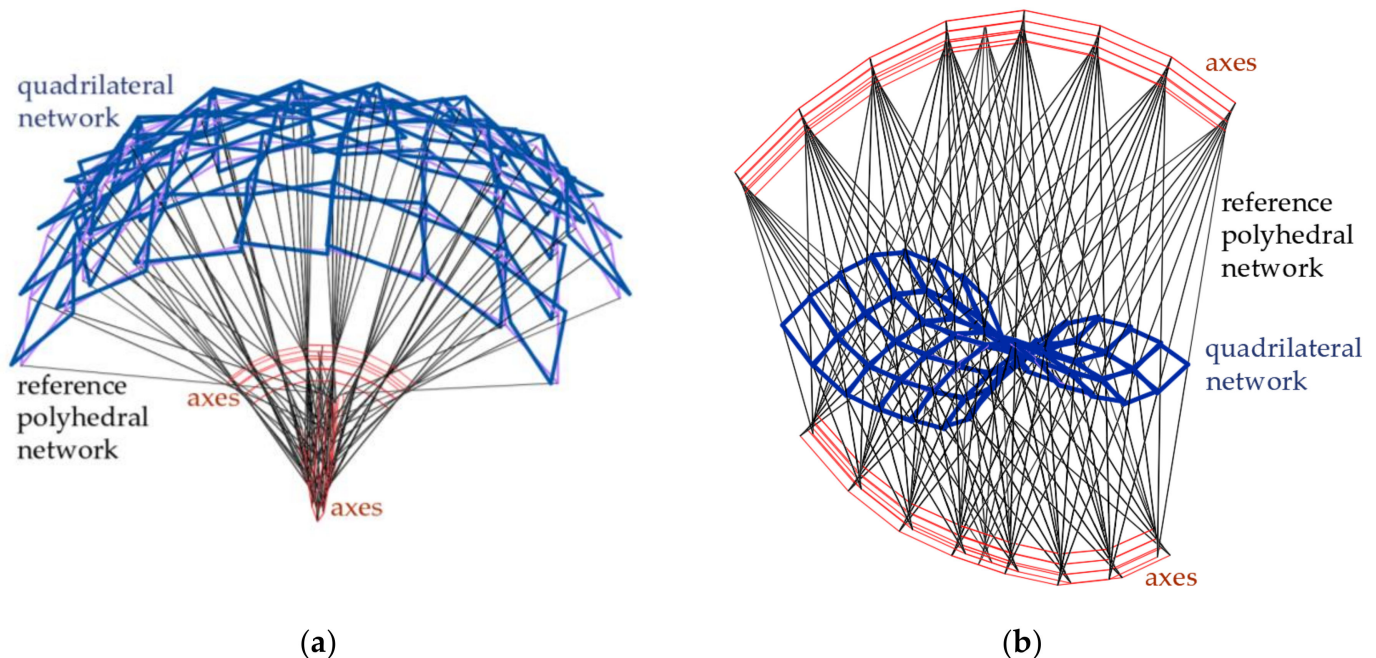
Figure 22. Two shell roof structures with eaves meshes arranged compatible with a regular surface of characterized by: (**a**) the positive Gaussian curvature, (**b**) the negative Gaussian curvature defined by means of two various polyhedral reference networks.

The third basic goal realized by means of the method is attractiveness and rationality of the final complex building free forms $\sum$, which is associated with the properties of the investigated networks Γ and B_v, and surface ω_r. The main elements determining the attractiveness are: (1) the ω_r's curvature in two orthogonal and diagonal directions, (2) the positions of the Γ's planes, and (3) the positions of the B_v's vertices on the Γ's side edges with respect to ω_r. Modifications of these elements enable us to maintain the expected shape and slope of the designed multi-plane facades and multi-segment shell roof structure, as well as their geometric coherence with the entire building free form.

The main elements determining the rationality of the investigated geometric structures are: (1) the mutual consistency and regular arrangement of all individual forms $\sum_{ij}$, (2) the mutual consistency and the regular arrangement of all individual roof forms Ω_{ij}, (3) the consistency of the entire roof and facade forms, (4) the regularity of the distribution of all Γ_{ij} relative to ω_r, and (5) the location of the contraction of each effectively transformed fold along its length, induced by the mutual position and slope of the B_{vij}'s and Ω_{ij}'s directrices. The rationality is defined by means of the respective division coefficients or proportions between the selected elements of the investigated networks and structures.

8. Conclusions

The investigated innovative method's algorithm utilizing the novel polyhedral reference networks for shaping unconventional visually attractive and shaped rational multi sector shell roofs, entire building free forms and their structural systems is proposed. The nominally plane thin-walled corrugated sheets transformed elastically and effectively into ruled shell shapes are the basic material impacting the shapes of the building elements.

The meshes of the reference networks enable the designer to define the eaves lines of all individual roof shell sectors made up of these sheets. The side edges and planes of these networks also define the elevations of the designed building free forms. Since

the roof directrices of the complete roof shell sectors are skew straight or curved lines, it is convenient to contain them in the planes of the reference networks. Many innovative systems of such planes separating the roof shell sectors and containing the eaves lines including directrices of the shell sectors can simply and intuitively be developed as polyhedral reference networks Γ using computer technology, including the novel applications written for the CAD systems.

The investigated parameterization, regularity, symmetry and intuitiveness of the engineering computational models created with the help of the novel algorithm and its implementation in the novel computer applications enables one to shape attractive and rational building free-forms. The complex nature of the investigated building free forms and many interdisciplinary problems, as well as the proposed iterative diversified solutions of many complete issues, require the use of computer technology to obtain optimal solutions.

The attractiveness of the presented method results from the freedom of shaping of the diversified shell roof structures characterized by the positive, negative and zero Gaussian curvature and various patterns of many complete shell segments in the roof depending on the adopted values of the analyzed division coefficients related to the investigated reference networks Γ and eaves nets B_v. Unlike other conventional methods, the extensive method for parametric shaping of the regular roof shell structures composed of many transformed corrugated shell sectors is developed based on the division coefficients. The regular shell units determined with B_v are used as an orthotropic material for composing the innovative roof structures. In addition, the method's algorithm takes account of the rectangular shapes of the folded sheets and the rational shape transformations of the shell units.

Institutional Review Board Statement: Not applicable.

Informed Consent Statement: Not applicable.

Data Availability Statement: Data is contained partially within the article and partially in the author's article: Abramczyk, J. Symmetric Free Form Building Structures Arranged Regularly on Smooth Surfaces with Polyhedral Nets. *Symmetry* **2020**, *12*, 763.

Conflicts of Interest: The author declares no conflict of interest. The funders had no role in the design of the study; in the collection, analyses, or interpretation of data; in the writing of the manuscript, or in the decision to publish the results.

Appendix A

Table A1. The coordinates of the vertices W_{ABij}, W_{CDij}, W_{ADij}, W_{BCij} (for i, j = 1, 2, 3) of the polyhedral reference network Γ_1.

Point	x-Coordinate (mm)	y-Coordinate (mm)	z-Coordinate (mm)
W_{AB13}	3254.30	0	468.2
W_{CD13}	5572.70	0	1487.4
W_{AD13}	−435.4	−1054.60	12,007.10
W_{BC13}	−435.4	1054.60	12,007.10
W_{AB21}	−1100.00	−87.2	−996.2
W_{CD21}	1100.00	−87.2	−996.2
W_{AD21}	−4500.00	−4880.70	55,786.90
W_{BC21}	0	2574.00	9677.1
W_{AB31}	−1210.00	−353.3	−2063.50

Table A1. *Cont.*

Point	x-Coordinate (mm)	y-Coordinate (mm)	z-Coordinate (mm)
W_{CD31}	1210.00	353.3	−2063.50
W_{AD31}	0	2574.00	9677.1
W_{BC31}	0	4374.60	9074.60
W_{AB23}	3589.70	−95.9	−580.8
W_{CD23}	6173.60	−105.5	435.5
W_{AD23}	−435.4	1054.60	12,007.10
W_{BC23}	−480	3133.70	11,876.90
W_{AB32}	1210.00	353.3	−2063.50
W_{CD32}	3959.70	−389.5	−1713.3
W_{AD32}	−110	2840.10	10,744.40
W_{BC32}	−121	4847.40	10,188.40
W_{AB33}	3959.70	−389.5	−1713.3
W_{CD33}	6838.90	−429.4	−708.6
W_{AD33}	−480	3133.70	11,876.90
W_{BC33}	−529.1	5371.00	11,378.60

Table A2. The coordinates of the points S_{Aij}, S_{Bij}, S_{Cij}, S_{Dij} (for i, j = 1, 2, 3) of the reference surface network ω_r.

Point	x-Coordinate (mm)	y-Coordinate (mm)	z-Coordinate (mm)
S_{A11}	4500.00	−4793.60	54,790.70
S_{B11}	4500.00	4880.70	55,786.90
S_{C11}	−4500.00	4793.60	54,790.70
S_{D11}	−4500.00	−4880.70	55,786.90
S_{A12}	−4500.00	−4880.70	55,786.90
S_{B12}	−4500.00	4793.60	54,790.70
S_{C12}	−13,517.10	4793.60	52,918.00
S_{D12}	−13,517.10	−4793.60	52,918.00
S_{A13}	−13,517.10	−4793.60	52,918.00
S_{B13}	−13,517.10	4793.60	52,918.00
S_{C13}	−21,737.10	4793.60	49,304.20
S_{D13}	−21,737.10	−4793.60	49,304.20
S_{A21}	4500.00	4880.70	55,786.90
S_{B21}	4500.00	13,460.50	53,340.40
S_{C21}	−4500.00	13,460.50	53,340.40
S_{D21}	−4500.00	4793.60	54,790.70
S_{A31}	4500.00	13,460.50	53,340.40
S_{B31}	4500.00	21,957.50	50,497.30
S_{C31}	−4500.00	21,957.50	50,497.30
S_{D31}	−4500.00	13,460.50	53,340.40
S_{A22}	−4500.00	4793.60	54,790.70
S_{B22}	xS_{C21}	13,460.50	53,340.40
S_{C22}	−13,675.60	13,605.30	52,270.20
S_{D22}	−13,517.10	4793.60	52,918.00
S_{A23}	−13,517.10	4793.60	52,918.00
S_{B23}	−13,675.60	13,605.30	52,270.20
S_{C23}	−22,104.00	13,660.90	49,061.50
S_{D23}	−21,737.10	4793.60	49,304.20
S_{A32}	−4500.00	13,460.50	53,340.40
S_{B32}	−4500.00	21,957.50	50,497.30
S_{C32}	−13,692.40	22,263.80	49,770.70
S_{D32}	−13,675.60	13,605.30	52,270.20
S_{A33}	−13,675.60	13,605.30	52,270.20
S_{B33}	−13,692.40	22,263.80	49,770.70
S_{C33}	−22,428.40	22,611.20	47,304.50
S_{D33}	−22,104.00	13,660.90	49,061.50

Table A3. The coordinates of the vertices A_{ij}, B_{ij}, C_{ij}, D_{ij} (for i, j = 1, 2, 3) of the eaves edge net B_{v1}.

Point	x-Coordinate (mm)	y-Coordinate (mm)	z-Coordinate (mm)
A_{11}	4400	−4706.4	53,794.50
B_{11}	4600	4880.7	55,786.90
C_{11}	−4400.0	4706.4	53,794.50
D_{11}	−4600.0	−4880.7	55,786.90
A_{12}	−4390.0	−4697.7	53,694.90
B_{12}	−4610.0	4889.4	55,886.50
C_{12}	−13,517.1	4697.9	51,869.00
D_{12}	−13,852.6	−4889.4	53,967.00
A_{13}	−13,148.2	−4688.1	51,764.10
B_{13}	−13,886.1	4899	54,071.90
C_{13}	−21,136.3	4688.1	48,252.20
D_{13}	−22,338.0	−4899.0	50,356.20
A_{21}	4390	4697.7	53,694.90
B_{21}	4610	13,726.60	54,407.70
C_{21}	−4390.0	13,194.40	52,273.00
D_{21}	−4610.0	4889.4	55,886.50
A_{31}	4379	13,167.70	52,166.30
B_{31}	4621	22,430.30	51,611.1
C_{31}	−4379.0	21,484.70	49,383.50
D_{31}	−4621.0	13,753.20	54,514.40
A_{22}	−4400.0	4706.4	53,794.50
B_{22}	−4621.0	13,753.20	54,514.40
C_{22}	−13,367.3	13,360.70	51,326.40
D_{22}	−13,886.1	4899	54,071.90
A_{23}	−13,517.1	4697.9	51,869.00
B_{23}	−13,983.9	13,850.00	53,213.90
C_{23}	−21,549.5	13,391.00	48,108.10
D_{23}	−22,338.0	4899	50,356.20
A_{32}	−4390.0	13,194.40	52,273.00
B_{32}	−4621.0	22,430.30	51,611.10
C_{32}	−13,352.3	21,827.40	48,778.90
D_{32}	−13,983.9	13,850.00	53,213.90
A_{33}	−13,367.3	13,360.70	51,326.40
B_{33}	−14,032.4	22,700.20	50,762.60
C_{33}	−21,916.7	22,208.40	46,465.10
D_{33}	−22,658.4	13,930.90	50,015.00

References

1. Abramczyk, J. *Shell Free Forms of Buildings Roofed with Transformed Corrugated Sheeting, Monograph*; Publishing House of Rzeszow University of Technology: Rzeszów, Poland, 2017.
2. Reichhart, A. *Geometrical and Structural Shaping Building Shells Made up of Transformed Flat Folded Sheets*; House of Rzeszow University of Technology: Rzeszów, Poland, 2002. (In Polish)
3. Prokopska, A.; Abramczyk, J. Responsive Parametric Building Free Forms Determined by Their Elastically Transformed Steel Shell Roofs Sheeting. *Buildings* **2019**, *9*, 46. [CrossRef]
4. Prokopska, A.; Abramczyk, J. Symmetric Shape Transformations of Folded Shell Roofs Determining Creative and Rational Shaping of Building Free Forms. *Symmetry* **2019**, *11*, 1438.
5. Abramczyk, J. Shape transformations of folded sheets providing shell free forms for roofing. In Proceedings of the 11th Conference on Shell Structures Theory and Applications, Gdańsk, Poland, 11–13 October 2017; Pietraszkiewicz, W., Witkowski, W., Eds.; CRC Press Taylor and Francis Group: London, UK, 2017; pp. 409–412.
6. Bathe, K.J. *Finite Element Procedures*; Prentice Hall: Englewood Cliffs, NJ, USA, 1996.
7. Nilson, V.E. Testing a light gauge steel hyperbolic paraboloid shell. *Proc. ASCE J. Struct. Div.* **1962**, *88*, 51–66. [CrossRef]
8. Winter, G. Strength of thin steel compression flanges. *Trans. ASCE* **1974**, *112*, 895–912.
9. McDermott, J.F. Single layer corrugated steel sheet hypars. *Proc. ASCE J. Struct. Div.* **1968**, *94*, 1279–1294. [CrossRef]
10. Egger, H.; Fischer, M.; Resinger, F. Hyperschale aus Profilblechen. *Stahlbau* **1971**, *12*, 353–361.
11. Gergely, P.; Banavalkar, P.V.; Parker, J.E. The analysis and behavior of thin-steel hyperbolic paraboloid shells. In *A Research Project Sponsored by the America Iron and Steel Institute*; Report No. 338; Cornell University: Ithaca, NY, USA, 1971.

12. Petcu, V.; Gioncu, D. Corrugated hypar structures. In Proceedings of the I International Conference on Lightweight Structures in Civil Engineering, Warsaw, Poland, 1 December 1995; pp. 637–644.
13. Davis, J.M.; Bryan, E.R. *Manual of Stressed Skin Diaphragm Design*; Granada Publishing Ltd.: London, UK, 1982.
14. Biswas, M.; Iffland, J.S.B. Metal decks used to form hypar-shell panels. In Proceedings of the 2nd Speciality Conference on Cold-Formed Steel Structures, Rolla, MO, USA, 15–17 August 1973.
15. Reichhart, A. Corrugated Deformed Steel Sheets as Material for Shells. In Proceedings of the International Conference on Lightweight Structures in Civil Engineering, Warsaw, Poland, 25–29 September 1995; pp. 625–636.
16. Grey, A. *Modern Differential Geometry of Curves and Surfaces with Mathematica*; CRC Press LCC: Boca Raton, FL, USA, 1999.
17. Abramczyk, J. Parametric shaping of consistent architectural forms for buildings roofed with corrugated shell sheeting. *J. Archit. Civil Eng. Environ.* **2017**, *10*, 5–18.
18. Prokopska, A.; Abramczyk, J. Innovative systems of corrugated shells rationalizing the design and erection processes for free building forms. *J. Archit. Civil Eng. Environ.* **2017**, *7*, 29–40. [CrossRef]
19. Abramczyk, J. Principles of geometrical shaping effective shell structures forms. *JCEEA* **2014**, *61*, 5–21. [CrossRef]
20. Abramczyk, J. Innovative Building Forms Determined by Orthotropic Properties of Folded Sheets Transformed into Roof Shells. *JASS* **2020**, *61*, 111–124.
21. Carmo, M.P. *Differential Geometry of Curves and Surfaces*; Prentice-Hall, Inc.: Englewood Cliffs, NJ, USA, 1976.
22. Abramczyk, J. Symmetric Free Form Building Structures Arranged Regularly on Smooth Surfaces with Polyhedral Nets. *Symmetry* **2020**, *12*, 763. [CrossRef]
23. Prokopska, A.; Abramczyk, J. Parametric Creative Design of Building Free Forms Roofed with Transformed Shells Introducing Architect's and Civil Engineer's Responsible Artistic Concepts. *Buildings* **2019**, *9*, 58.
24. Abel, J.F.; Mungan, I. *Fifty Years of Progress for Shell and Spatial Structures*; International Association for Shell and Spatial Structures: Madrid, Spain, 2011.
25. Saitoh, M. *Recent Spatial Structures in Japan*; J. JASS: Madrid, Spain, 2001.
26. Obrębski, J.B. Observations on Rational Designing of Space Structures. In Proceedings of the Symposium Montpellier Shell and Spatial Structures for Models to Realization IASS, Montpellier, France, 20–24 September 2004; pp. 24–25.
27. Rębielak, J. Morphology of roof structure systems designer by means of lenticular girder. In *Spatial Structures–Temporary and Permanent, Proceedings of the International Symposium of the International Association for Shell and Spatial Structures, Shanghai, China, 8–12 November 2010*; Zhang, Q., Yang, L., Hu, Y., Eds.; China Architecture & Building Press: Shanghai, China, 2010; pp. 1249–1256.
28. Reichhart, A. Principles of designing shells of profiled steel sheets. In Proceedings of the X International Conference on Lightweight Structures in Civil Engineering, Rzeszow, Poland, 5–6 December 2004; pp. 138–145.
29. Wei-Wen Yu, P.E. *Cold Formed Steel Design*; John Wiley and Sons Inc.: New York, NY, USA, 2000.
30. Samyn, P.P. Structures isobarres et isonoeuds. In Proceedings of the 2nd International Conference on Space Structures—University of Surrey, Guilford, UK, 11–14 September 1975; pp. 621–634.
31. Pottmann, H.; Kilian, A.; Hofer, M. Advances in Architectural Geometry. In Proceedings of the AAG Conference, Vienna, Austria, 13–16 September 2008.
32. Pottmann, H.; Asperi, A.; Kilian, A.; Hofer, M. *Architectural Geometry*; Bentley, Institute Press: Exton, PA, USA, 2007.
33. Żwirek, P. Selected issues of using nominally flat folded sheets and self-bearing panels for curved. In Proceedings of the 9th Scientific and Technical Conference on Shaping Structures. Thin-walled Structures, Rzeszów, Poland, 11–12 September 2015. (In Polish).
34. Abbas, I.; Marin, M.; Saeed, T. A GL model on thermo-elastic interaction in a poroelastic material using finite element method. *Symmetry* **2020**, *12*, 488.
35. Craciun, E.M.; Marin, M.; Pop, N. Some Results in Green–Lindsay Thermoelasticity of Bodies with Dipolar Structure. *Mathematics* **2020**, *8*, 497.
36. Sharma, A. Urban greenways: Operationalizing design syntax and integrating mathematics and science in design. *Front. Archit. Res.* **2015**, *4*, 24–34. [CrossRef]
37. Hasgül, E. Space as configuration: Patterns of space and culture. In Proceedings of the ARCHTHEO 2015—9th Conference: Theory and History of Architecture, Istanbul, Turkey, 5–7 November 2015.
38. Eekhout, M. Form as a Bridge between Architectural, Structural and Industrial Design. In Proceedings of the 4th International Colloqium on Structural Morphology IASS: Spatial Lattice and Tension Structures, Delft, The Netherlands, 15 March 2000; pp. 1000–1010.
39. Wester, T. The Nature of Structural Morphology. In Proceedings of the IASS Symposium: Spatial Lattice and Tension Structures, Atlanta, GA, USA, 24–28 April 1994; pp. 1000–1010.
40. Qingpeng, L. *Form Follows Force: A Theoretical Framework for Structural Morphology, and Form-Finding Research on Shell Structures*; *Monograph*; Delft University of Technology: Delft, The Netherlands, 2018.